DAFTAR PUSTAKA

Avicenna M.F., Sufriadin., Budiman A.A., dan Widodo S., 2019., Analisis Mineralogi dan Kualitas Batubara Desa Kadingeh, Kecamatan Baraka, Kabupaten Enrekang, Sulawesi Selatan, *Jurnal Geomine*, Vol. 7, No. 2, hal. 114-123.

Anggayana K., Darijanto T., dan Widodo S., 2003, Studi pirit sebagai sumber sulfur pada batubara. *Jurnal JTM FIKTM ITB*, Vol. 10, No. 1, hal. 1-14.

Annisa., 2016, Pengaruh Mineral Sekunder Sulfat Hasil Oksidasi Pirit Terhadap Nilai Total Sulfur Pada Batubara Formasi Haloq dan Serpih Karbonan Formasi Batuayau Cekungan Kutai Atas. *Promine Journal,* Vol. 4, No. 2, hal. 31-376.

Anshariah,, Imran A,M,, Widodo S,, and Irvan U,R,, 2020, Correlation of total sulfur content to the percentage of pyrite content by microscopy in Mallawa formation coal, South Sulawesi Province, Indonesia, *IOP Conference Series: Earth and Environmental Science, Volume 575, The 2nd International Conference of Interdisciplinary Research on Green Environmental Approach for Sustainable Development 25 June 2020, Gedung Pasca Sarjana, Indonesia,* pp, 1-7,

ASTM D388., 2019, Standard Classification of Coals by Rank, *ASTM Book of Standards*, Vol. 05.06, ASTM Internasional, West Conshohocken, PA, 8 p.

ASTM D3172., 2013*, Standard Practice for Proximate Analysis of Coal and Coke*, Vol. 05.06, ASTM Internasional, West Conshohocken, PA, 2 p.

ASTM D3174., 2018, *Standard Test Method for Ash in the Analysis Sample of Coal and Coke from Coal*, Vol. 05.06, ASTM Internasional, West Conshohocken, PA, 6 p.

ASTM D3176., 2015, *Standard Practice for Ultimate Analysis of Coal and Coke*, Vol. 05.06, ASTM Internasional, West Conshohocken, PA, 4 p.

ASTM D4239., 2018, *Standard Test Method for Sulfur in the Analysis Sample of Coal and Coke Using High-Temperature Tube Furnace Combustion*, Vol. 05.06, ASTM Internasional, West Conshohocken, PA, 8 p.

ASTM D5373., 2021, *Standard Test Methods for Determination of Carbon, Hydrogen and Nitrogen in Analysis Samples of Coal and Carbon in Analysis Samples of Coal and Coke*, Vol. 05.06, ASTM Internasional, West Conshohocken, PA, 11 p.

Bhattacharya J.P., 2006, Deltas. In: Posamentier, H.W., Walker, R.G. (Eds.), Facies Models Revised. *SEPM Special Publication, vol. 84.* pp. 237–292.

Baihaqi A., Susilawati R., Fauzielly L., dan Muljana B., 2017, Studi Perbandingan Karakteristik Kimia dan Petrografi Batubara Lapangan X, Cekungan Sumatera Selatan dan Lapangan Y Cekungan Sumatera Tengah Indonesia, *Buletin Sumber Daya Geologi*, Vol. 12, No. 2, hal. 87-102.

Brahmantyo B., dan Bandono., 2006, Klasifikasi Bentuk Muka Bumi (Landform) untuk Pemetaan Geomorfologi pada Skala 1:25,000 dan Aplikasinya untuk Penataan Ruang, *Jurnal Geoaplika,* Vol. 1, No. 2, hal. 71-78.

Calvert S.J., 1999, The Cenozoic Evolution of the Lariang and Karama Basins, Sulawesi. *Proceeding of the IPA*, pp. 505-511.

Casagrande D.J., Siefert K., Berschinski C., and Sutton N., 1977, Sulfur in peat-forming system of the Okefenokee swamp and Florida everglades : Origins of sulfur in coal, *Geochimica et Cosmochimica* 44, pp. 161-167.

Chayes F., 1956, *Petrografic Modal Analysis*, John Wiley & Sons, New York, 133 p.

Chou C.L., 2012, sulfur in coals: A review of geochemistry and origins, *International Journal of Coal Geology,* Vol. 100, pp. 1-13.

Cohen A.D., Andrejko M.J., Spackman W., Corvinus D., 1984, Peat deposits of the Okefenokee Swamp. In: *Cohen A.D., Casagrande D.J., Andrejko M.J., Best G.R. (Eds.), The Okefenokee Swamp: Its Natural History, Geology and Geochemistry. Wetland Surveys, Los Alamos, N.M.,* pp. 493–553.

Cohen A.D., Gage C.P., Moore W.S., 1999a, Combining organic petrography and palynology to assess anthropogenic impacts on peatlands: Part 1. An example from the northern Everglades of Florida, *Int. J. Coal Geol* 39, pp. 3–45.

Cohen A.D., Gage C.P., Moore W.S., VanPelt R.S., 1999b, Combining organic petrography and palynology to assess anthropogenic impacts on peatlands: Part 2. An example from a Carolina Bay wetland at the Savannah River Site in South Carolina, *Int. J. Coal Geol* 39, pp. 47–95.

Coleman J.M., and Prior D.B., 1982, Deltaic environments of deposition. In: Scholle, P.A., Spearing, D.R. (Eds.), Sandstone Depositional Environments. *American Association of Petroleum Geologists Memoir*, vol. 31, pp. 139–178.

Craig J.R., and Vaughan D.J., 1981, *Ore Microscopy and Ore Petrography*, John Wiley and Sons, New York, 25p.

Dai S., Bechtel A., Eble C.F, Flores R.M., French D., Graham I.T., Hood M.M., Hower J.C., Korasidis V.A., Moore T.A., Püttmann W., Wei Q., Zhao L., and O'Keefe J.M.K., 2020, Recognition of peat depositional environments in coal: A review, *International Journal of Coal Geology. 219,* pp. 1-67.

Demchuk T.D., 1992, Epigenetic pyrite in a low- sulphur, sub-bituminous coal from the central Alberta Plains, *International ournal of Coal Geology 21*, pp. 187–196.

Diessel C.F.K., 1986, On the Correlation between Coal Facies and Depositional Environments. *Proceeding of 20th Symposium of Department of Geology*, *University Newcastle*, N.S.W, pp. 19-22.

Diessel C.F.K., 1992, *Coal-Bearing Depositional System*, Springer-Verlag. Berlin, Heidelberg, 728 p.

Edress N.A.A., and Sykorova I., ,2007, Haquebard's Double Triangle and its role to reconstruct paleohydrologic regime and vegetation zones of peat conditions in planar-mire systems, *General View ICCP News*, Vol 42, pp. 42-46.

Elliott T., 1986, Deltas. In: Sedimentary Environments And Facies. *Blackwell Scientific Publications, Oxford, U.K,* pp. 113–154.

Falcon R.M.S., and Snyman C.P., 1986, *An Introduction to Coal Petrography Atlas of Petrographic Constituents in the Bituminous Coals of Southern Africa*, Johannesburg : Geological Society of South Africa*,* 27 p.

Flores R.M., 2014, *Coal and Coalbed Gas*: Fueling the future. Elsevier, Amsterdam,720 p.

Horne J.C., Ferm J.C., Caruccio F.T., and Baganz B.P., 1978, Depositional models in coal exploration and mine planning in Appalachian region, *Bulletin of the American Association of Petroleum Geologists* 62, pp. 2379-2411.

Huda M., Salinita S., dan Ningrum N.S., 2017, Perubahan Komposisi Maseral Dalam Batubara Wahau Setelah Proses Pengeringan/Upgrading, *Jurnal Teknologi Mineral dan Batubara*, Vol. 13, No. 3, hal. 225-235.

Ibrahim M.A., dan Fatimah., 2015, Penyelidikan Batubara Daerah Bonehau dan Sekitarnya, Kabupaten Mamuju, Provinsi Sulawesi Barat, *Kelompok Penyelidikan Batubara, Pusat Sumber Daya Geologi,* hal. 1-10.

International Committee for Coal and Organic Petrology (ICCP)., 2001, The New Inertinite Classification (ICCP System 1994), *Fuel 80*, pp. 459-471.

Kalkreuth W.D., Marchioni D.L., Calder J.H., Lamberson M.N., Naylor R.D., and Paul J., 1991, The relationship between coal petrography and depositional environments from selected coal basins in Canada, *International Journal of Coal Geology,* Vol. 19, pp. 21-76.

Kemezys M., Taylor,G.H., 1964, Occurrence and distribution of minerals in some Australian coals. *J. Inst. Fuel 37*, pp. 389–397.

Khan D., Qiu L., Liang C., Mirza K, Rehman S.U., Han Y., Hannan A., Kashif M., and Kra K.L., 2022, Genesis and Distribution of Pyrite in the Lacustrine Shale: Evidence from the Es3x Shale of the Eocene Shahejie Formation, Zhanhua Sag, East China, *ACS Omega,* Vol. 7, (1) , pp. 1244-1258.

Lamberson M.N., Bustin R.M., and Kalkreuth W., 1991, Lithotype (Maceral) Composition and Variation as Correlated with Paleo wetland Environments, Gates Formations, Northeastern British Columbia, Canada. *International Journal of Coal Geology,* Vol. 18, pp. 87-12.

Liu M., Peizhen W., Simin C., and Dailin Z., 2019, The Classification of Inertinite Macerals in Coal Based on the Multifractal Spectrum Method, *Applied Sciences 9*, no. 24: 5509, pp. 1-16.

Loye H.Z., 2013, *X-Ray Diffraction-How It works, What It Can, and What It Can Not Tell Us. Handout ppt*, University of South Carolina, Caroline. 34 p.

Mackowsky M, TH., 1982, *Minerals and trace elements occurring in coal*. (In *Stach, E et al: Stach's Texbook of Coal Petrology*), Gebruder Borntraeger, Berlin. 153-170 p.

Martini I.P., Glooschenko W., 1984, *Cold climate environments of peat formation in Canada*. Adv Stud Syd Bas, 18 Newcastle Symp Proc, pp 18-28.

Miller K., 2013, Coal analysis, in Osborne, D. (ed.), *The coal handbook : Towards Cleaner Production 1st Edition,* Woodhead Publishing Limited, Swaston, Cambridge, pp. 151-189.

Monita A.P., Aryanto N.C.D., dan Ashar Y., 2021, Kajian Lingkungan Pengendapan Batubara Berdasarkan Analisis Petrografi Organik pada Formasi Muara Enim, Cekungan Sumatera Selatan, *Jurnal Teknologi Mineral dan Batubara*, Vol. 17, No. 3, hal. 123-133.

Moore P.D., 1987, Ecological and hydrological aspects of peat formation. In: Coal and Coal-Bearing Strata: Recent Advances. *Geological Society Special Publication 32*, pp. 7–15.

Moore T.A., Shearer J.C., Miller S.L., 1996a, Fungal origin of oxidized plant material in the Palangkaraya peat deposit, Kalimantan Tengah, Indonesia: Implications of inertinite`formation in coal, *Int. J. Coal Geol* 30, pp. 1–23.

Moore T.A., Shearer J.C., Miller S.L., 1996b, Fungal origin of oxidised plant material inthe Palangkaraya peat deposit, Kalimantan Tengah, Indonesia: Implications for "inertinite"formation in coal, *Int. J. Coal Geol* 30, pp. 1–23.

Nursanto E., Idrus A., Amijaya H., dan Pramumijoyo S., 2011, Keterdapatan dan Tipe Mineral Pada Batubara Serta Metode Analisisnya. *Jurnal Teknologi Technoscientia,* Vol. 4, No. 1, hal. 1-10.

Ogala J., Siavalas G., and Christanis K., 2012, Coal petrography, mineralogy and geochemistry of lignite samples from the Ogwashi–Asaba Formation, Nigeria. *Journal of African Earth Sciences,* Vol. 66-67, pp. 35-45.

O'Keefe J.M.K., Bechtel A., Christanis K., Dai S., DiMichele W., Eble C.F., Ward C.R., Esterle J.S., Mastalerz M., Raymond A.L., Valentim B.V., Wagner N.J., and Hower J.C., 2013, On the fundamental difference between coal rank and coal type, *International Journal of Coal Geology,* Vol. 118, pp. 58-87.

Pajares J.A., and Díez M.A., 2014, Coal and coke. In: Reedijk, J. (ed.), *Encyclopedia reference module in chemistry, molecular sciences and chemical engineering*. Elsevier, Waltham, MA, pp. 173-192.

Pasymi., 2008, *Batubara (Jilid 1),* Bung Hatta University Press, Sumatera, Indonesia, 95 p.

Permana A., Ward C.R., Li Z., Gurba L.W., 2013, Distribution and origin of minerals in high-rank coals of the South Walker Creek area, Bowen Basin, Australia. *Int. J. Coal Geol. 116-117*, pp. 185–207.

Permana A., Ward C.R., Li Z., Gurba L.W., 2014, Maceral Characteristics and Vitrinite Reflectance Variation of The High Rank Coals, South Walker Creek, Bowen Basin, Australia. *Indonesian Journal on Geoscience.* Vol. 8, pp 63-74.

Pickel W., Kus J., Flores D., Kalaizidis S., Christanis K., Cardott B.J., Misz-Kennan M., Rodrigues S., Hentschel A., Hamor-Vido M., Crosdale P., and Wagner N., ICCP., 2017, Classification of liptinite – ICCP System 1994, *Int. J. Coal Geol* 169, pp. 40–61.

Purnama A.B., Salinita S., Sudirman, Sendjaja Y.A., dan Muljana B., 2018, Penentuan Lingkungan Pengendapan Lapisan Batubara D, Formasi Muara Enim, Blok Suban Burung, Cekungan Sumatera Selatan, *Jurnal Teknologi Mineral dan Batubara*, Vol. 14, hal. 1-18.

Pratama M.F., Sjafri1 I., Gani1 R.M.G., Firmansyah Y., Suwarna N., 2020, Kondisi Lingkungan Pengendapan, Kematangan, dan Klasifikasi Batubara Berdasarkan Data Petrografi dan Geokimia Organik, Lapangan Rokan Hulu, *Padjadjaran Geoscience Journal*. Vol. 4, No. 1, hal. 92-106.

Posamentier, H.W., Jervey, M.T., Vail, P.R., 1988. Eustatic controls on clastic deposition I–conceptual framework. In: Sea-Level Changes: An Integrated Approach. *Spec. publ. Soc. Econ. Paleontol. Mineral 42,* pp. 109–124.

Qadaryati N., Praditya D.T., Hidajat, W.K., dan Martiningtyas I., 2019, Penentuan Lingkungan Pengendapan Batubara Berdasarkan Karakteristik dan Maseral Batubara di PT X, Kabupaten Nunukan, Kalimantan Utara, *Jurnal Geosains dan Teknologi,* Vol. 2, No. 3, hal. 107-116.

Ranton J.J., 1982, *Mineral matter* in Coal, In Meyer R.A, Coal Structure, *Academic Press, London*, pp. 283-324.

Rao C.P., and Gluskoter, H.J., 1973. Occurrence and Distribution of Minerals in Illinois Coals. *Illinois State Geological Survey, Circular* 476, pp 1-56.

Salinita S., dan Bahtiar A., 2014, Pengaruh Struktur Geologi Terhadap Kualitas Batubara Lapisan "D" Formasi Muara Enim, *Jurnal Teknologi Mineral dan Batubara,* Vol. 10, No. 2, hal. 91-104.

Sari S.L., Rahmawati M.A., Triyoga A., and Idarwati., 2017, Impact of Sulphur Content on Coal Quality at Delta Plain Depositional Environment: Case study in Geramat District Lahat Regency, South Sumatra, *Journal of*

Geoscience, Engineering, Environment, and Technology, Vol. 2, (3), pp. 1-8.

Scott A.C., 2002, Coal petrology and the origin of coal macerals: a way ahead?, *International Journal of Coal Geology* 50 (1–4), pp. 119-134.

Speight J.G., 2015, *Handbook Of Coal Analysis Second Edition,* John Wiley & Sons, Hoboken, New Jersey, 365 p.

Stach E., Mackowsky M.T., Teichmüller M., Taylor G.H., Chandra D. and Teichmüller R., 1982, *Stach's textbook of coal petrology*, Gebruder Borntraeger, Berlin. 535 p.

Speight J.G., 2013, *The Chemistry and Technology of Coal (3rd ed.)*. CRC Press. Boca Raton, Amerika Serikat. 845 p.

Sufriadin, Widodo S, dan Mendaun Y., 2016, Analisis Petrografi dan Kualitas Batubara Sinjai, Sulawesi Selatan. *Jurnal Penelitian Enjiniring,* Vol. 20, No. 2, hal. 21-25.

Suharyana., 2012, *Dasar-Dasar dan dan Pemanfaatan Metode Difraksi Sinar X.* Universitas Sebelas Maret. Surakarta.

Sykorova I., Pickel W., Christanis K., Wolf M., Taylor G.H., and Flores D., 2005, Classification of huminite (ICCP System 1994), *International Journal of Coal Geology 62*, p. 85-106.

Rahim F.A., Sjafri I., Gani R.M.G., dan Suwarna N., 2018, Karakteristik dan Lingkungan Pengendapan Batubara Formasi Purukcahu Berdasarkan Analisis Petrografi, di Daerah Murung Raya, Kalimantan Tengah, *Padjadjaran Geoscience Journal,* Vol. 2, No. 4, hal. 259-268.

Rahmad B., Sugeng., Ediyanto., Daryono S.K., Putra G.P., Simatupang I., and Rahman M.R., 2020, Sclerotinia Maceral Analysis to Predict Facies Condition on Coal of Muara Enim Formation, Marapi Area, Lahat, South Sumatera, *LPPM UPN "Veteran" Yogyakarta Conference Series Proceeding on Engineering and Science Series (ESS),* Vol. 1, No. 1, pp. 656-668.

Taliding T.U., Widodo S., Ilyas A., Sufriadin S., Anas A.V., and Irfan U.R., 2022, Vertical Distribution of Total Sulfur in Coal Seams in Tamalea Village, Bonehau Regency, West Sulawesi Province. *International Journal of Engineering and Science Applications*, Vol. 9, No. 1, pp 25-32.

Taylor G.H., Teichmüller M., Davis A., Diessel C.F.K., Robert P., and Littke R., 1998, *Organic Petrology*, Berlin, Stuttgart: GebrüderBorntraeger, 704 p.

Teichmüller M., 1989, The genesis of coal from the viewpoint of coal petrology, *International Journal of Coal Geology*, 12 (1–4) , pp. 1–87.

Thomas L., 2012, *Coal Geology Second Edtion,* John Wiley & Sons, Ltd, Chichester, 472 p.

Ting F.T.C., 1977, Origin and Spacing of Coal Bends*, Journal of Pressure Vessel Technology,* 99, pp. 624-626.

Toprak S., Sutcu E.C., and Senguler I., 2015, A fault controlled, newly discovered Eskişehir Alpu coal basin in Turkey, its petrographical properties and depositional environment, *International Journal of Coal Geology,* Vol. 138*,* pp. 127-144.

UN-ECE., 1998, *International Classification of in-Seam Coals*. Economic Commission for Europe, Committee on Sustainable Energy, Geneva, 41 p.

Van Krevelen D.W., 1981, *Coal : Typology, Chemistry, Phisics, Constitution. – 2nd ed,* Elsevier, Amsterdam, 514 p.

Ward C.R., 1984, Coal Geology and Coal Technology, Blackwell Scientific Publications, Oxford, 345 pp.

Ward C.R., 1986, Review of *mineral matter* in coal. *Aust. Coal Geol*, pp. 87–110.

Ward C.R., 1989. Minerals in bituminous coals of the Sydney Basin (Australia) and the Illinois Basin (U.S.A.). *Int. J. Coal Geol.* Vol. 13, pp. 455–479.

Ward C.R., 2002, Analysis and significance of mineral matter in coal seams. *Int. J. Coal Geol*. 50, pp. 135–168.

Ward C.R., 2016, Analysis, origin and significance of mineral matter in coal: an updated review. *Int. J. Coal Geol*. 165, pp. 1–27.

Widayat A.H., 2005, *Hubungan interpretasi fasies dan lingkungan pengendapan batubara dengan variasi sulfur seam R dan Q, Sub-Cekungan Berau, Cekungan Tarakan, Kalimantan Timur*, Tesis Magister, TeknikPertambangan, Fakultas Teknik Pertambangan dan Perminyakan, Institut Teknologi Bandung.

Widodo S., Oschwann W., Bechtel A., Sachsenhofer R.F., Anggayana K., and Puettmann W., 2010, Distribution of Sulfur and Pyrite in Coal Seam from Kutai Basin (East Kalimantan, Indonesia): Implication for Paleoenvironmental Conditions, *International Journal Coal Geology*, Vol. 81, pp. 151-162.

Widodo, S., dan Antika, R. (2012). Studi Fasies Pengendapan Batubara Berdasarkan Komposisi Maseral di Kabupaten Barru Sulawesi Selatan. *Prosiding Hasil Penelitian Fakultas Teknik Vol. 6,* Universitas Hasanuddin, Gowa, hal. 1-10.

Widodo S., Sufriadin, Imai A., and Anggayana K., 2016, Characterization of Some Coal Deposits Quality by Use of Proximate and Sulfur Analysis in the Southern Arm Sulawesi, Indonesia, *International Journal of Engineering and Science Applications*, Vol. 3, pp. 137-143.

Widodo S., Sufriadin., Ansyariah, Budiman A.A., Asmiani N., Jafar N., dan Babay MF., 2019, Karakterisasi Mineral Pirit Pada Batubara Berdasarkan Hasil Analisis Mikroskopi, Proksimat, Total Sulfur, dan Difraksi Sinar X: Potensi Terjadinya Air Asam Tambang. *Jurnal GEOSAPTA*, Vol. 5, No. 2, hal. 121-126.

Widodo S., Sufriadin., Thamrin M., Wahyufirmansyah., and Jafar N., 2020, Mineralogy and quality of Banti Coal, Baraka District, Enrekang Regency, South Sulawesi Province, Indonesia. *IOP Conference Series: Earth and Environmental Science, Volume 473, The 2nd International Conference on Global Issue for infrastructure, environment & socio-economic development 12-13 September 2019, South Sulawesi, Indonesia,* pp. 1-9.

Win C.T., Surjono S.S., Amijaya D.H., Husein S., Aihara A., and Watanabe K., 2013, Distribution of pyrite and *mineral matter* in coal seams from Samarinda Area, Lower Kutai Basin, Indonesia. *Clean Coal Technology*, pp.17-24.

Xie P., Song H., Wei J., and Li Q., 2016, Mineralogical Characteristics of Late Permian Coals from the Yueliangtian Coal Mine, Guizhou, Southwestern China, *Minerals,* Vol. 6, (29), pp. 1-21.

Zheng X., Wang Z., Wang L., Xu Y., and Liu J., 2017, Mineralogical and Geochemical Compositions of the Lopingian Coals and Carbonaceous Rocks in the Shugentian Coalfield, Yunnan, China:with Emphasis on Fe-Bearing Minerals ina Continental-Marine Transitional Environment, *Minerals,* Vol. 7, (170), pp. 1-25.

Zhu Q., 2014, *Coal Sampling And Analysis Standards,* IEA Clean Coal Centre, London, United Kingdom, 123 p.

LAMPIRAN

Lampiran A. Peta situasi lokasi penelitian

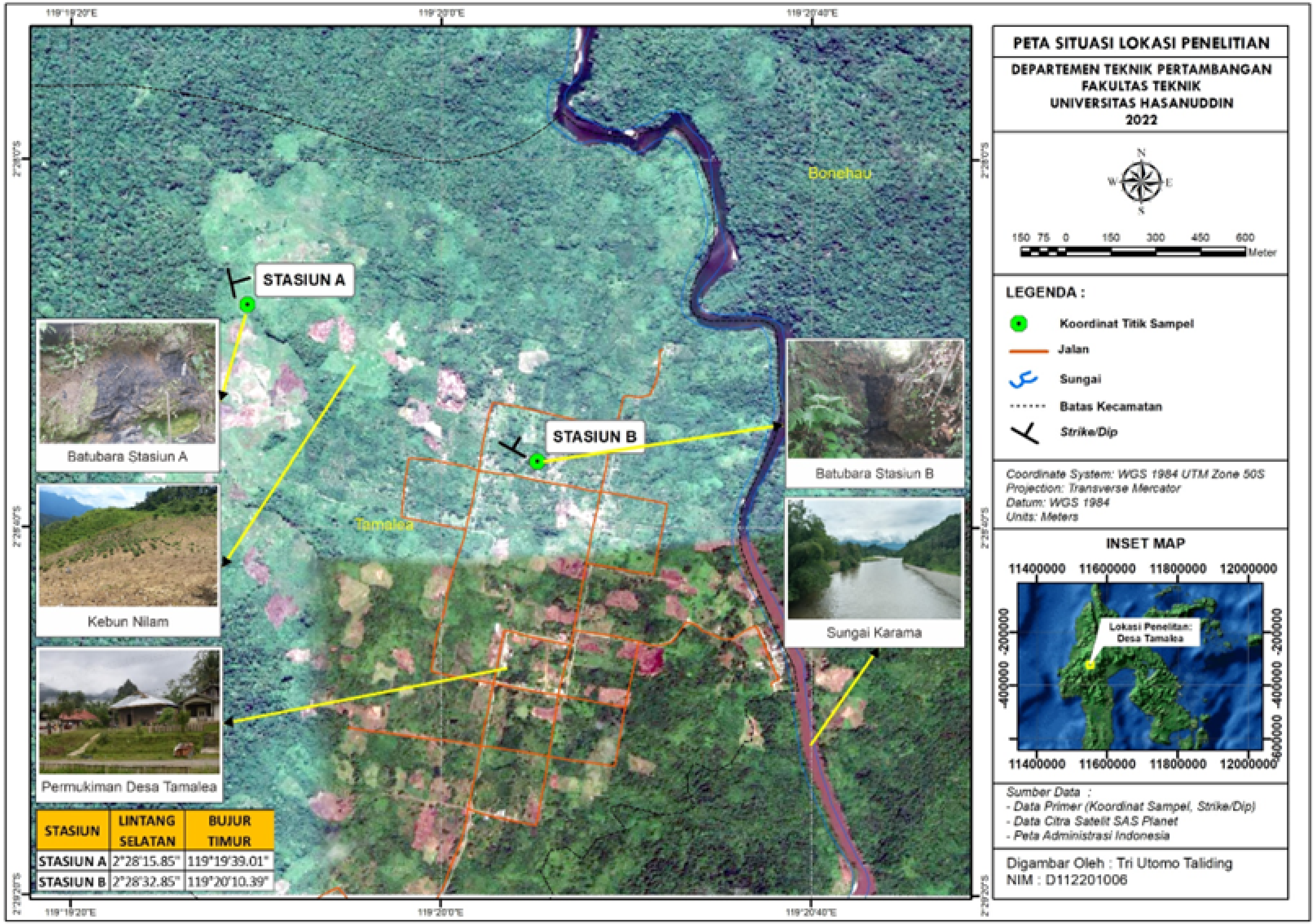

Lampiran B. Dokumentasi Penelitian

Lampiran C. Laporan hasil analisis proksimat

LABORATORIUM ANALISIS DAN PENGOLAHAN BAHAN GALIAN
DEPARTEMEN TEKNIK PERTAMBANGAN
UNIVERSITAS HASANUDDIN

Hasil Analisis Proksimat

Kode Sampel	Kadar Air	Kandungan Abu	Zat Terbang	Karbon Tetap
	(%) ar	(%) ar	(%) ar	(%) ar
BNH01_PL01	8,36	5,49	62,83	23,32
BNH01_PL02	4,89	38,01	23,27	33,83
BNH02_PL01	8,42	5,80	39,02	46,76
BNH02_PL02	3,65	64,96	17,69	13,70

Analisis proksimat dilakukan menggunakan standar ASTM D3172-13.

Gowa, 11 Oktober 2021

Laboran

Akmal Saputno, ST

Lampiran D. Laporan hasil analisis nilai kalori dan total sulfur batubara

SUCOFINDO
Kantor Penerb
Jl. Urip Sumoharjo No. 90 A, Makasar 902
Telp./Faksimili: 0411 451890/4517
Email: makassar@sucofindo.co

LAPORAN ANALISIS

PELANGGAN	:	Tri Utomo Taliding Jl. Pongtiku, No. 29 , Kec. Mamuju , Kabupaten Mamuju Sulawesi Barat
SAMPEL	:	Batubara
ANALISIS / UJI	:	Total Sulfur dan Nilai Kalori
TANGGAL TERIMA	:	28/10/2021
TANGGAL ANALISA	:	28/10/2021
DESKRIPSI SAMPEL	:	Bentuk : Bubuk Berat : ± 5 gram

Hasil:

Kode Sampel	Parameter	Satuan	Hasil	Metode
BNH 01 PL 01	Total Sulfur	%	0,6648	ASTM D – 4239 – 2018
	Kalori	KCal/Kg	6733,48	ASTM D – 5865 – 2013
BNH 01 PL 02	Total Sulfur	%	2,2698	ASTM D – 4239 – 2018
	Kalori	KCal/Kg	4888,67	ASTM D – 5865 – 2013
BNH 02 PL 01	Total Sulfur	%	1,2978	ASTM D – 4239 – 2018
	Kalori	KCal/Kg	6394,78	ASTM D – 5865 – 2013
BNH 02 PL 02	Total Sulfur	%	4,4471	ASTM D – 4239 – 2018
	Kalori	KCal/Kg	2643,74	ASTM D – 5865 – 2013

HASIL ANALISA TERSEBUT DIATAS HANYA MERUJUK PADA SAMPLE YANG DISERAHKAN DIMANA PENGAMBILAN SAMPLE TERSEBUT TIDAK DILAKUKAN OLEH SUCOFINDO

Bidang Inspeksi & Pengujian

SUCOFINDO
Achmad

Lampiran E. Konversi nilai kalori batubara Kcal/Kg ke Btu/Lb

1. Konversi nilai kalori sampel BNH01_PL01

$$GCV_{im,MMf} = \frac{100(GCV_{im} - 50S_m)}{(100 - (1{,}08A_{im} + 0{,}55S_{im}))}$$

$$GCV_{im,MMf} = \frac{100(6733{,}48 - 50\ x\ 0{,}86)}{(100 - (1{,}08\ x\ 5{,}49 + 0{,}55\ x\ 0{,}86))}$$

$$GCV_{im,MMf} = \frac{100\ x\ 6690{,}48}{100 - 6{,}4022}$$

$$GCV_{im,MMf} = \frac{669048}{93{,}5978}$$

$$GCV_{im,MMf} = 7148{,}12\ Kcal/Kg$$

$$GCV_{im,MMf} = 12866{,}61\ Btu/Lb$$

2. Konversi nilai kalori sampel BNH01_PL02

$$GCV_{im,MMf} = \frac{100(GCV_{im} - 50S_m)}{(100 - (1{,}08A_{im} + 0{,}55S_{im}))}$$

$$GCV_{im,MMf} = \frac{100(4888{,}67 - 50\ x\ 2{,}27)}{(100 - (1{,}08\ x\ 38{,}01 + 0{,}55\ x\ 2{,}27))}$$

$$GCV_{im,MMf} = \frac{100\ x\ 4775{,}17}{100 - 42{,}2993}$$

$$GCV_{im,MMf} = \frac{477517}{57{,}7007}$$

$$GCV_{im,MMf} = 8275{,}76\ Kcal/Kg$$

$$GCV_{im,MMf} = 14896{,}36\ Btu/Lb$$

3. Konversi nilai kalori sampel BNH01_PL02

$$GCV_{im,MMf} = \frac{100(GCV_{im} - 50S_m)}{(100 - (1{,}08A_{im} + 0{,}55S_{im}))}$$

$$GCV_{im,MMf} = \frac{100(6394{,}78 - 50\ x\ 1{,}3)}{(100 - (1{,}08\ x\ 5{,}8 + 0{,}55\ x\ 1{,}3))}$$

$$GCV_{im,MMf} = \frac{100\ x\ 6329{,}78}{100 - 6{,}979}$$

$$GCV_{im,MMf} = \frac{632978}{93{,}021}$$

$$GCV_{im,MMf} = 6804{,}68\ Kcal/Kg$$

$$GCV_{im,MMf} = 12248{,}42\ Btu/Lb$$

4. Konversi nilai kalori sampel BNH01_PL02

$$GCV_{im,MMf} = \frac{100(GCV_{im} - 50S_m)}{(100 - (1{,}08A_{im} + 0{,}55S_{im}))}$$

$$GCV_{im,MMf} = \frac{100(263{,}74 - 50\ x\ 4{,}45)}{(100 - (1{,}08\ x\ 64{,}96 + 0{,}55\ x\ 4{,}45))}$$

$$GCV_{im,MMf} = \frac{100\ x\ 2421{,}24}{100 - 72{,}6043}$$

$$GCV_{im,MMf} = \frac{242124}{27{,}3957}$$

$$GCV_{im,MMf} = 8838{,}03\ Kcal/Kg$$

$$GCV_{im,MMf} = 15908{,}45\ Btu/Lb$$

Stasiun	Kode Sampel	Kalori. Ar (Kcal/Kg)	Rata-Rata Kalori. Ar (Kcal/Kg)	Kcal/Kg ke Btu/Lb	Rata-Rata Kalori. Ar (Btu/Lb)	Rata-Rata Kalori. Im,mmf (Btu/Lb)
Stasiun A	BNH01-PL01	6733,48	5811,08	1,80	10459,94	13881,49
	BNH01-PL02	4888,67				
Stasiun B	BNH02-PL01	6394,78	4519,26	1,80	8134,67	14078,44
	BNH02-PL02	2643,74				
Rata-rata		5165,17	5165,17	1,80	9297,30	13979,96

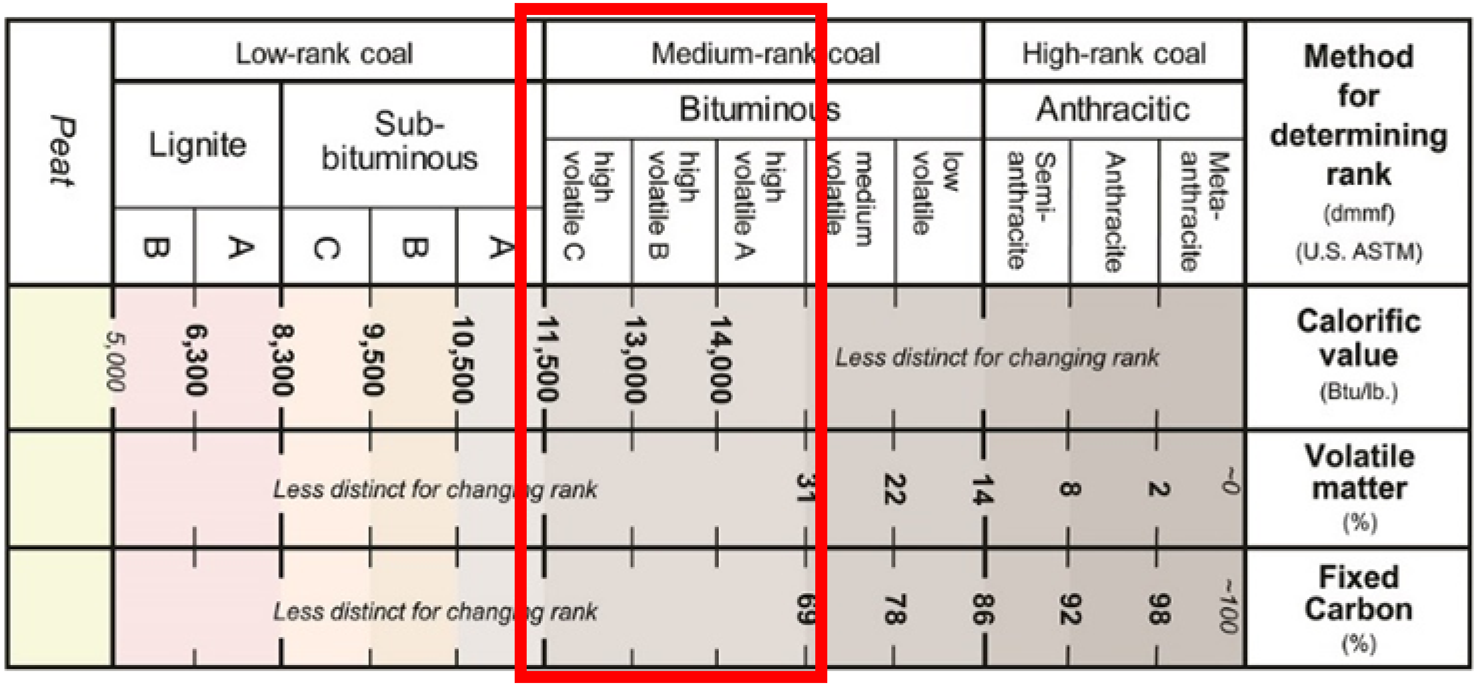

Lampiran F. Laporan hasil analisis total sulfur batuan pengapit (overburden dan underburden)

SUCOFINDO
Kantor Penerbit:
Jl. Urip Sumoharjo No. 90 A, Makasar 90232
Telp./Faksimili: 0411 451890/451796
Email: makassar@sucofindo.co.id

LAPORAN ANALISIS

PELANGGAN	:	Tri Utomo Taliding Jl. Pongtiku, No. 29 , Kec. Mamuju , Kabupaten Mamuju Sulawesi Barat
SAMPEL	:	BATU LEMPUNG
ANALISIS / UJI	:	TOTAL SULFUR, AR %
TANGGAL TERIMA	:	28/10/2021
TANGGAL ANALISA	:	28/10/2021 to 31/10/2021
DESKRIPSI SAMPEL	:	Bentuk : Bubuk Berat : ± 5 gram

Hasil:

Kode Sampel	Satuan	Hasil	Metode
BNH01_RF	%	0,22716	ASTM D – 4239 - 2018
BNH01_FL	%	3,85350	ASTM D – 4239 – 2018
BNH02_RF	%	0,19901	ASTM D – 4239 – 2018
BNH02_FL	%	5,79770	ASTM D – 4239 – 2018

HASIL ANALISA TERSEBUT DIATAS HANYA MERUJUK PADA SAMPLE YANG DISERAHKAN DIMANA PENGAMBILAN SAMPLE TERSEBUT TIDAK DILAKUKAN OLEH SUCOFINDO

Bidang Inspeksi & Pengujian

SUCOFINDO

Achmad

Lampiran G. Hasil analisis mikroskopis sampel BNH01_PL01 menggunakan Nikon Eclispse LV1*0*

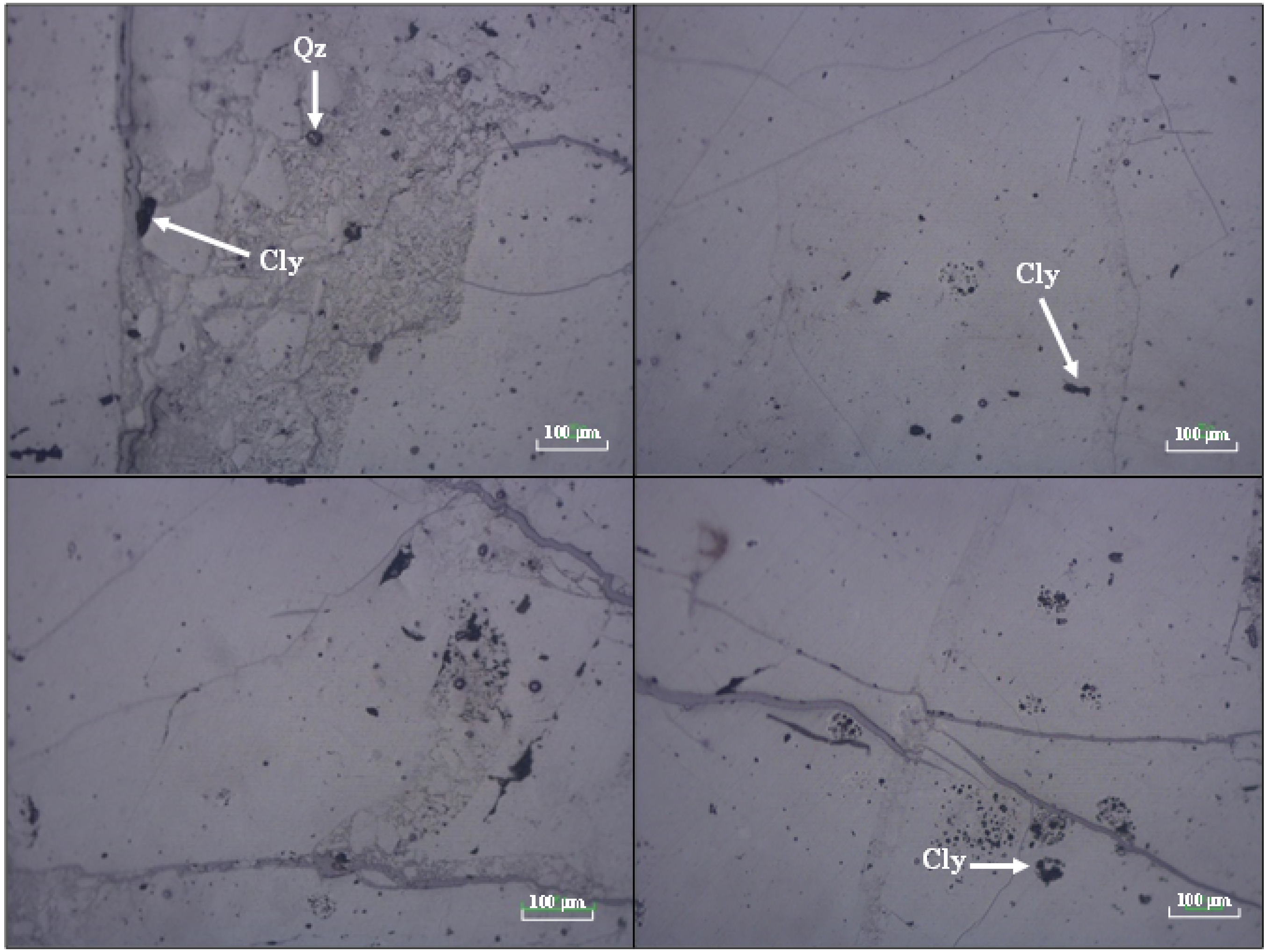

Lampiran H. Hasil analisis mikroskopis sampel BNH01_PL02 menggunakan Nikon Eclipse LV10

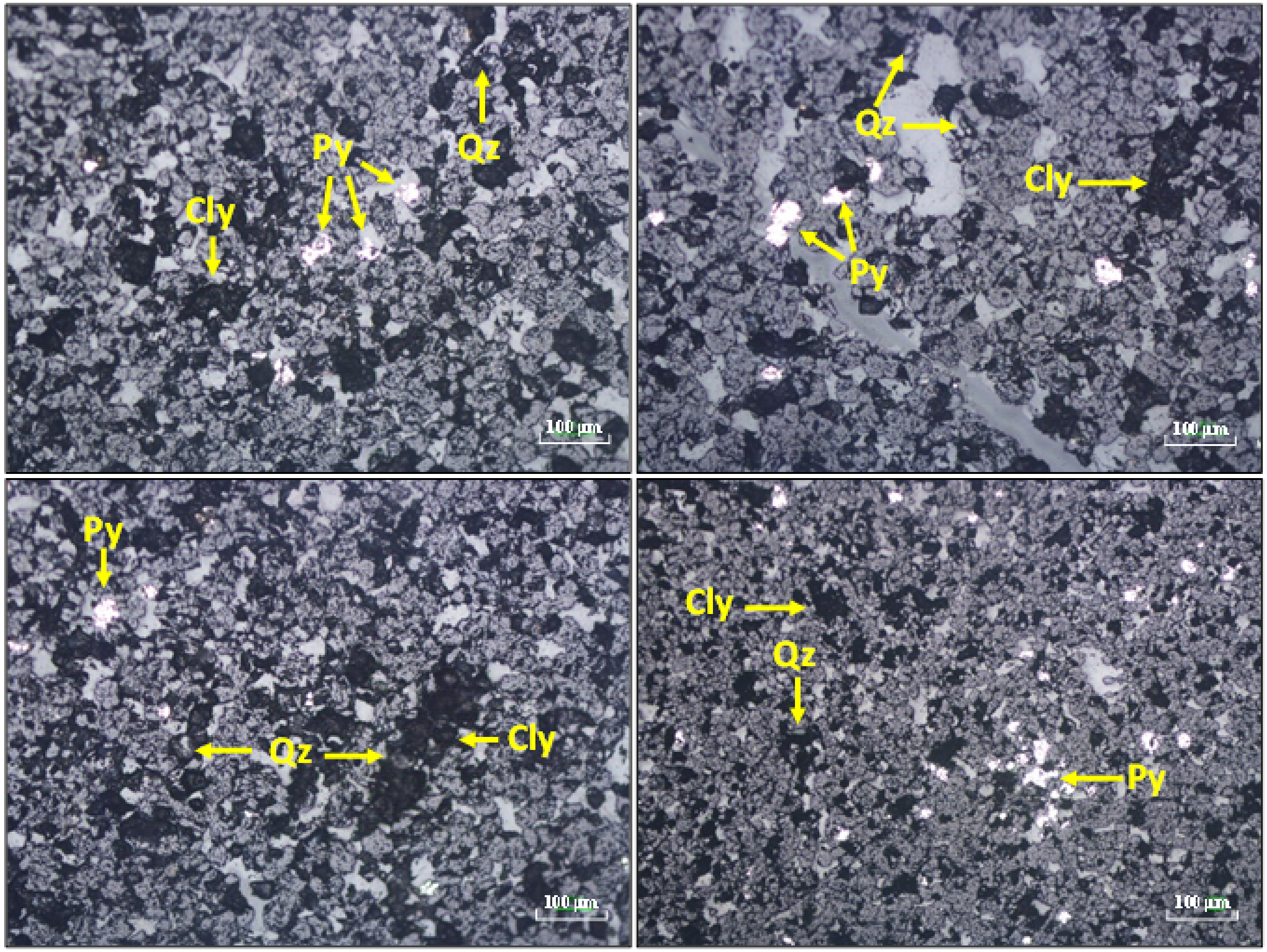

Lampiran I. Hasil analisis mikroskopis sampel BNH02_PL01 menggunakan Nikon Eclispse LV10

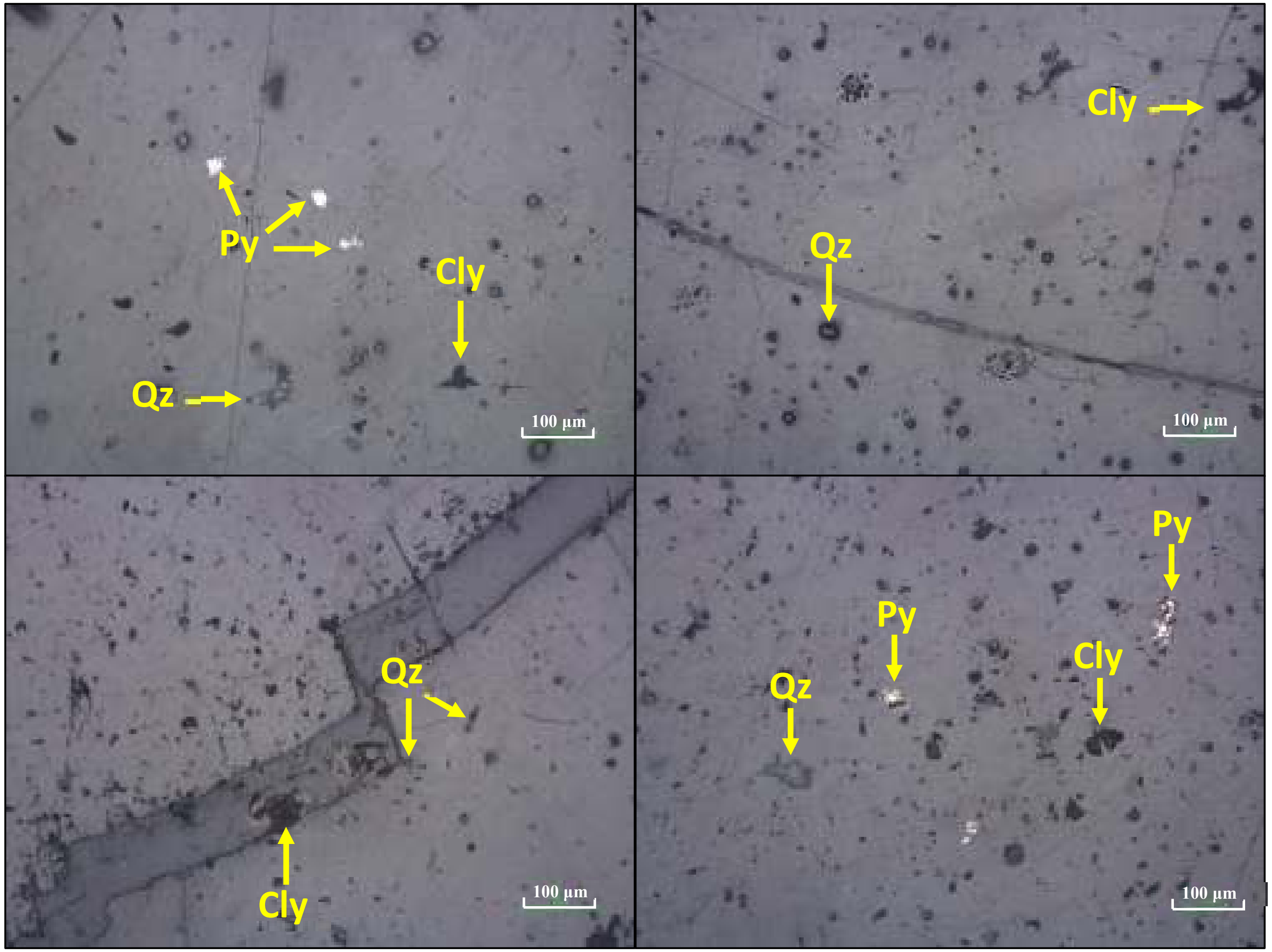

Lampiran J. Hasil analisis mikroskopis sampel BNH02_PL02 menggunakan Nikon Eclispse LV10

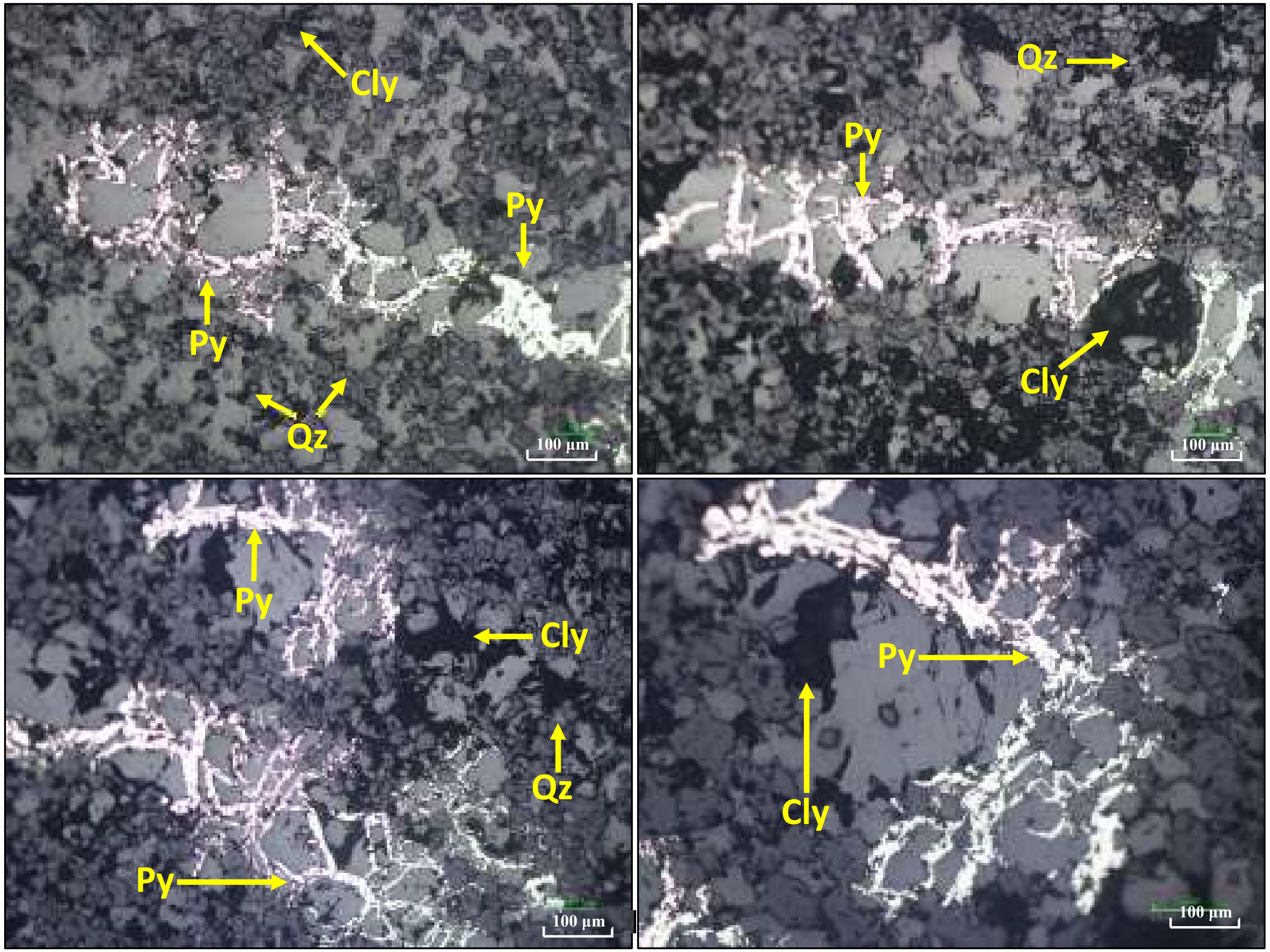

Lampiran K. Laporan hasil analisis X-Ray Diffraction (XRD) sampel BNH01_PL01

Match! Phase Analysis Report

Sample: BNH01-PL01 (5-70)

Sample Data

File name	BNH01-PL01.RAW
File path	F:/PASCA SARJANA TAMBANG UNHAS/02. Proposal/02. Analisa/02. Hasil Analisa/05. XRD/XRD BNH/BNH01-PL01
Data collected	Feb 8, 2022 13:15:38
Data range	5.000° - 70.000°
Original data range	5.000° - 70.000°
Number of points	3251
Step size	0.020
Rietveld refinement converged	No
Alpha2 subtracted	No
Background subtr.	No
Data smoothed	Yes
Radiation	X-rays
Wavelength	1.540600 Å

Analysis Results

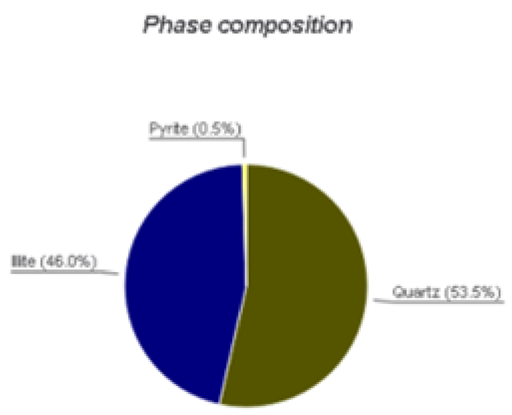

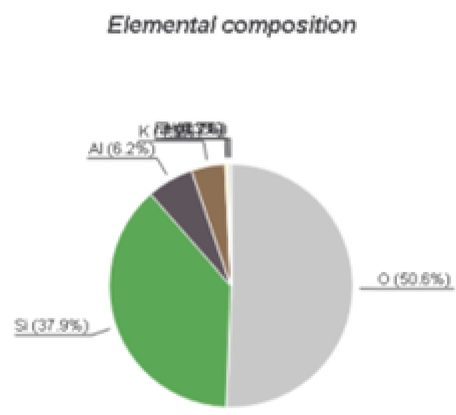

Index	Amount (%)	Name	Formula sum
A	53.5	Quartz	O2 Si
B	46.0	Illite	Al2 H2 K O12 Si4
C	0.5	Pyrite	Fe S2
	18.7	*Unidentified peak area*	

Amounts calculated by RIR (Reference Intensity Ratio) method after manual adjustment of intensity scaling factor(s)

Element	Amount (weight %)
O	50.6%(*)
Si	37.9%
Al	6.2%
K	4.5%
S	0.3%
Fe	0.2%
H	0.2%(*)
*LE (sum)	50.8%

Details of identified phases

A: Quartz (53.5 %)

Formula sum	O2 Si
Entry number	96-900-9667
Figure-of-Merit (FoM)	0.867943
Total number of peaks	70
Peaks in range	70
Peaks matched	18
Intensity scale factor	0.83
Space group	P 31 2 1
Crystal system	trigonal (hexagonal axes)
Unit cell	a= 4.9158 Å c= 5.4091 Å
I/Ic	2.84
Calc. density	2.644 g/cm³

Reference	Gualtieri A. F., "Accuracy of XRPD QPA using the combined Rietveld-RIR methodLocality: Baveno, Novara, Italy", Journal of Applied Crystallography **33**, 267-278 (2000)

B: Illite (46.0 %)

Formula sum	Al2 H2 K O12 Si4
Entry number	96-901-3723
Figure-of-Merit (FoM)	0.948649
Total number of peaks	303
Peaks in range	303
Peaks matched	110
Intensity scale factor	0.20
Space group	C 1 2/m 1
Crystal system	monoclinic
Unit cell	a= 5.2350 Å b= 9.0320 Å c= 10.1400 Å β= 101.520 °
I/Ic	0.79
Calc. density	2.824 g/cm³
Reference	Drits V. A., Zviagina B. B., McCarty D. K., Salyn A. L., "Factors responsible for crystal-chemical variations in the solid solutionsfrom illite to aluminoceladonite and from glauconite to celadoniteLocality: South Urals, RussiaSample Name: 60", American Mineralogist **95**, 348-361 (2010)

C: Pyrite (0.5 %)

Formula sum	Fe S2
Entry number	96-900-0596
Figure-of-Merit (FoM)	0.611518
Total number of peaks	33
Peaks in range	33
Peaks matched	14
Intensity scale factor	0.00
Space group	P 1
Crystal system	triclinic (anorthic)
Unit cell	a= 5.4166 Å b= 5.4166 Å c= 5.4166 Å α= 90.000° β= 90.000 ° γ= 90.000 °
I/Ic	0.99
Calc. density	5.015 g/cm³
Reference	Bayliss P., "Crystal structure refinement of a weakly anisotropic pyrite", American Mineralogist **62**, 1168-1172 (1977)

Candidates

Name	***Formula***	***Entry No.***	***FoM***
Silicon fluoride	F4 Si	96-101-0135	0.7262
Yttrium tantalum tungsten oxide (0.2/0.7/0.3/3)	O3 Ta0.72 W0.28 Y0.24	96-100-1125	0.7258
	B N	96-900-8998	0.7246
Thallium chloride	Cl Tl	96-101-1365	0.7201
	Mg Sm	96-152-3336	0.7200
	Be F2	96-153-1932	0.7155
	Cl Tl	96-900-8795	0.7109
Na0.11 (W O3)	Na0.11 O3 W	96-154-2049	0.7037
Graphite	C	96-900-0047	0.7034
	Mn3 Pt	96-152-2203	0.7009
(Fe0.14 Mn0.86)3 Pt	Fe0.42 Mn2.58 Pt	96-152-4750	0.7006
K.05 Tl.95 Cl	Cl K0.05 Tl0.95	96-154-1956	0.6949
	As4 O6	96-451-3285	0.6931
Lithium chloride hydrate	Cl H2 Li O	96-101-0496	0.6911
Na0.54 (W O3)	Na0.54 O3 W	96-154-1824	0.6894
Pretulite	O4 P0.952 Sc0.904 Si0.048 Y0.032 Yb0.016 Zr0.048	96-900-4707	0.6872
Gd S F	F Gd S	96-152-5881	0.6838
Co (N H3)6 I3	Co H18 I3 N6	96-711-7904	0.6818
	F1.6 Fe0.4 Zr0.1	96-901-5147	0.6814
Iron zirconium fluoride (0.8/0.2/3.2)	F3.2 Fe0.8 Zr0.2	96-100-8535	0.6814
Iron zirconium fluoride (0.8/0.2/3.2)	F3.2 Fe0.8 Zr0.2	96-100-8563	0.6814
	O7 P2 Si	96-591-0161	0.6809
Copper-tetracyanoborate	C4 B Cu N4	96-430-8584	0.6801
	Ag In S2	96-150-9401	0.6791
Mo O2.4 F0.6	F0.6 Mo O2.4	96-210-6057	0.6772
	As H6 N O4	96-154-5061	0.6738
hexagonal boron nitride	B N	96-201-6171	0.6734
	Li2 Mg2 Mo3 O12	96-720-4607	0.6730
Na.72 W O3	Na0.72 O3 W	96-412-4850	0.6724
Na.54 W O3	Na0.54 O3 W	96-412-4846	0.6715
	Cl O	96-901-4607	0.6709
Pretulite	O4 P Sc	96-900-1950	0.6673
Boron Nitride	B N	96-591-0080	0.6657
Li S H	H Li S	96-153-7484	0.6649
	Co Ga Sm	96-152-5271	0.6629
Trilithium aluminium trimolybdate(VI)	Al Li3 Mo3 O12	96-201-8503	0.6625
Tricaesium lithium dizinc tetrakis(tetraoxotungstate)	Cs3 Li O16 W4 Zn2	96-202-0924	0.6621

Genthelvite	Be3 O12 S Si3 Zn4	96-900-0951	0.6609
Chlorine	Cl2	96-901-3123	0.6608
Li3 Fe (Mo O4)3	Fe Li3 Mo3 O12	96-152-7652	0.6588
	F4 K Y	96-702-0656	0.6571
Tl3 Ta S4	S4 Ta Tl3	96-231-0549	0.6569
(La1.75 Sr0.25) Ni O4.036	La1.75 Ni O14 Sr0.25	96-703-5744	0.6541
	Cu In Se	96-410-5294	0.6540
	Ca F5 Ti	96-154-5630	0.6540
	Nb O3	96-901-5166	0.6538
Hydrogen niobium oxide	H Nb O3	96-100-0190	0.6532
Hydrogen niobium oxide	H Nb O3	96-100-0191	0.6532
Niobic acid	H Nb O3	96-100-0402	0.6532
Sc P O4	O4 P Sc	96-231-0639	0.6531
	Gd Mg	96-152-2528	0.6527
Rb2 K (Bi F6)	Bi F6 K Rb2	96-152-5838	0.6525

and 273 others...

Search-Match

Settings

Reference database used	COD-Inorg 2022.06.29
Automatic zeropoint adaptation	Yes
Downgrade entries with low scaling factors	Yes
Minimum figure-of-merit (FoM)	0.60
2theta window for peak corr.	0.30 deg.
Minimum rel. int. for peak corr.	0
Parameter/influence 2theta	0.50
Parameter/influence intensities	0.50
Parameter multiple/single phase(s)	0.50

Criteria for entries added by user

Reference:

Entry number: 96-101-0914;96-101-0930;96-101-0941;96-154-4892;96-154-4893;96-154-4894;96-210-4742;96-210-4743;96-210-4753;96-210-4754;96-500-0116;96-724-2111;96-900-0110;96-900-0595;96-900-0596;96-900-6171;96-900-6172;96-900-7573;96-901-0012;96-901-3070;96-901-3071;96-901-3072;96-901-3409;96-901-3698;96-901-5006;96-901-5235;96-901-5637;96-901-5843;96-901-6640;96-900-1665;96-900-3815;96-900-4787;96-900-4919;96-900-7429;96-900-7612;96-900-9523;96-900-9666;96-901-0118;96-901-0494;96-901-0549;96-901-1123;96-901-1745;96-901-1746;96-901-2893;96-901-3719;96-901-3720;96-901-3721;96-901-3722;96-901-3723;96-901-3724;96-901-3733;96-901-3985;96-901-4065;96-901-6664;96-101-1098;96-101-1160;96-101-1173;96-101-1177;96-101-1201;96-110-0020;96-500-0036;96-900-0776;96-900-0777;96-900-0778;96-900-0779;96-900-0780;96-900-0781;96-900-5018;96-900-5019;96-900-5020;96-900-5021;96-900-5022;96-900-5023;96-900-5024;96-900-5025;96-900-5026;96-900-5027;96-900-5028;96-900-5029;96-900-5030;96-900-5031;96-900-5032;96-900-5033;96-900-5034;96-900-7379;96-900-8093;96-900-8094;96-900-9667;96-901-0145;96-901-0146;96-901-0147;96-901-1494;96-901-1495;96-901-1496;96-901-1497;96-901-2601;96-901-2602;96-901-2603;96-901-2604;96-901-2605;96-901-2606;96-901-3322;96-901-5023

Peak List

No.	*2theta [°]*	*d [Å]*	*I/I0 (peak height)*	*Counts (peak area)*	*FWHM*	*Matched*
1	5.08	17.3817	9.41	6.30	0.4945	
2	8.89	9.9357	20.64	13.55	0.4845	B
3	16.35	5.4166	30.36	20.35	0.4945	C
4	17.84	4.9679	54.08	36.25	0.4945	B
5	19.64	4.5160	61.42	41.17	0.4945	B
6	19.89	4.4604	73.31	49.14	0.4945	B
7	20.34	4.3620	71.32	47.81	0.4945	B
8	20.85	4.2572	102.28	68.56	0.4945	A
9	21.60	4.1113	103.05	69.08	0.4945	B
10	23.20	3.8301	104.29	69.91	0.4945	C
11	23.22	3.8283	103.40	51.47	0.3673	B
12	24.37	3.6488	114.94	47.30	0.3036	B
13	26.62	3.3454	855.58	231.95	0.2000	A
14	26.65	3.3417	1000.00	329.73	0.2433	B
15	26.90	3.3119	135.04	234.29	1.2800	B
16	28.52	3.1273	4.80	1.56	0.2400	C
17	29.11	3.0649	24.63	22.36	0.6699	B
18	30.68	2.9121	6.86	9.92	1.0661	B
19	33.05	2.7083	14.07	2.29	0.1200	C
20	33.53	2.6707	11.12	3.53	0.2343	B
21	34.29	2.6128	0.31	0.10	0.2379	B
22	34.52	2.5965	6.98	1.14	0.1200	B
23	34.79	2.5766	0.61	0.10	0.1200	B

24	34.96	2.5648	8.56	1.79	0.1545	B
25	36.03	2.4907	1.63	0.26	0.1200	B
26	36.13	2.4839	14.59	2.37	0.1200	B
27	36.46	2.4622	64.12	34.27	0.3943	B
28	36.53	2.4579	82.95	36.62	0.3257	A
29	36.62	2.4522	80.75	28.15	0.2572	B
30	37.08	2.4224	4.70	0.76	0.1200	C
31	37.39	2.4030	0.82	0.13	0.1200	B
32	37.91	2.3714	0.61	0.10	0.1200	B
33	38.26	2.3505	1.88	0.84	0.3289	B
34	39.44	2.2828	28.47	10.68	0.2767	A
35	39.83	2.2616	2.20	0.67	0.2245	B
36	39.89	2.2580	6.45	1.51	0.1722	B
37	39.90	2.2578	6.77	1.34	0.1461	B
38	40.27	2.2377	25.61	11.04	0.3179	A
39	40.41	2.2302	18.05	11.98	0.4897	B
40	40.77	2.2113	8.21	1.34	0.1200	C
41	40.77	2.2112	8.35	1.36	0.1200	B
42	40.96	2.2018	19.22	4.12	0.1583	B
43	41.36	2.1810	8.18	1.54	0.1392	B
44	41.46	2.1764	67.83	11.91	0.1296	B
45	41.95	2.1517	20.75	3.38	0.1200	B
46	42.43	2.1286	58.16	18.88	0.2395	A
47	42.75	2.1134	22.73	3.70	0.1200	B
48	43.05	2.0995	3.69	0.72	0.1438	B
49	44.02	2.0556	62.43	11.16	0.1319	B
50	44.70	2.0257	6.22	1.06	0.1260	B
51	44.85	2.0195	3.52	0.59	0.1230	B
52	45.44	1.9944	11.42	1.86	0.1200	B
53	45.62	1.9871	64.17	10.44	0.1200	B
54	45.77	1.9807	25.99	2.57	0.0729	A
55	46.54	1.9499	16.68	5.43	0.2400	B
56	46.66	1.9450	1.91	0.46	0.1800	B
57	47.44	1.9150	4.71	0.77	0.1200	C
58	47.46	1.9142	3.13	0.51	0.1200	B
59	48.02	1.8930	9.52	4.53	0.3511	B
60	48.77	1.8656	2.40	0.39	0.1200	B
61	49.04	1.8563	0.43	0.10	0.1707	B
62	49.95	1.8244	12.34	2.01	0.1200	B
63	50.11	1.8190	0.36	0.10	0.2040	A
64	50.11	1.8188	116.65	18.97	0.1200	B
65	50.51	1.8055	49.92	8.12	0.1200	C
66	50.58	1.8030	1.88	0.67	0.2626	A
67	52.26	1.7490	43.32	8.54	0.1454	B
68	53.32	1.7169	4.22	0.69	0.1200	B
69	53.45	1.7129	5.55	0.90	0.1200	C
70	53.46	1.7127	0.61	0.10	0.1200	B
71	53.53	1.7106	4.25	0.69	0.1200	B
72	53.60	1.7084	0.61	0.10	0.1200	B
73	53.61	1.7082	0.61	0.10	0.1200	B
74	53.76	1.7038	1.15	0.19	0.1200	B
75	53.95	1.6982	0.61	0.10	0.1200	B
76	54.04	1.6956	0.61	0.10	0.1200	B
77	54.07	1.6948	0.61	0.10	0.1200	B
78	54.58	1.6800	4.13	0.67	0.1200	B
79	54.83	1.6729	39.63	6.45	0.1200	B
80	54.84	1.6727	1.27	0.42	0.2413	A
81	54.91	1.6708	0.61	0.10	0.1200	B
82	55.25	1.6612	5.78	0.94	0.1200	B
83	55.26	1.6611	0.57	0.10	0.1305	B
84	55.29	1.6603	0.09	0.01	0.1253	A
85	55.44	1.6559	3.97	0.65	0.1200	B
86	55.71	1.6486	1.31	0.21	0.1200	B
87	55.82	1.6455	0.55	0.09	0.1200	B
88	56.21	1.6353	0.61	0.10	0.1200	B
89	56.28	1.6332	2.51	0.41	0.1200	C
90	56.29	1.6331	0.61	0.10	0.1200	B
91	56.37	1.6310	2.49	0.40	0.1200	B
92	56.44	1.6291	2.46	0.40	0.1200	B
93	57.20	1.6091	5.96	0.74	0.0912	A
94	57.34	1.6055	13.19	2.15	0.1200	B
95	57.69	1.5966	0.61	0.10	0.1200	B
96	58.36	1.5798	0.31	0.10	0.2400	B
97	59.03	1.5636	14.49	2.36	0.1200	C
98	59.27	1.5577	5.22	0.85	0.1200	B
99	59.40	1.5547	2.81	0.46	0.1200	B

100	59.90	1.5430	81.82	13.31	0.1200	B
101	59.93	1.5423	14.05	10.83	0.5683	A
102	60.08	1.5388	89.55	14.57	0.1200	B
103	60.10	1.5382	0.61	0.10	0.1200	B
104	60.35	1.5324	11.67	3.80	0.2400	B
105	61.38	1.5093	14.67	2.39	0.1200	B
106	61.51	1.5063	55.25	8.99	0.1200	B
107	61.56	1.5053	8.18	1.33	0.1200	B
108	61.60	1.5044	7.84	1.27	0.1200	B
109	61.69	1.5023	6.16	1.00	0.1200	C
110	61.91	1.4976	14.55	2.37	0.1200	B
111	62.04	1.4948	11.04	1.80	0.1200	B
112	62.18	1.4917	7.15	1.16	0.1200	B
113	62.34	1.4883	0.61	0.10	0.1200	B
114	62.41	1.4868	0.61	0.10	0.1200	B
115	62.93	1.4758	0.24	0.13	0.4012	B
116	63.14	1.4713	3.85	2.07	0.3956	B
117	63.45	1.4649	3.99	2.13	0.3928	B
118	63.88	1.4560	7.47	3.96	0.3914	B
119	63.98	1.4540	9.71	5.14	0.3907	B
120	63.99	1.4538	16.63	9.73	0.3905	A
121	64.15	1.4507	8.20	4.34	0.3903	B
122	64.30	1.4476	4.01	2.12	0.3900	C
123	64.65	1.4406	13.73	7.26	0.3900	B
124	64.78	1.4379	18.54	9.80	0.3900	B
125	64.96	1.4344	2.76	1.46	0.3900	B
126	64.99	1.4339	0.62	0.33	0.3900	B
127	65.26	1.4286	1.64	0.87	0.3900	B
128	65.39	1.4260	7.75	4.10	0.3900	B
129	65.73	1.4194	6.10	3.22	0.3900	B
130	65.75	1.4191	5.93	2.26	0.2550	A
131	67.19	1.3921	1.86	0.30	0.1200	B
132	67.52	1.3862	13.79	17.19	0.9198	B
133	67.70	1.3828	22.30	26.30	0.7873	A
134	67.71	1.3827	25.42	22.57	0.6549	B
135	68.10	1.3758	33.95	29.93	0.5886	A
136	68.28	1.3726	32.89	27.36	0.5555	A
137	68.40	1.3704	31.21	22.10	0.5224	B
138	68.42	1.3701	28.85	17.84	0.4562	B
139	68.80	1.3635	4.28	2.46	0.4231	B
140	68.85	1.3625	5.08	2.86	0.4148	B
141	68.94	1.3609	9.40	5.13	0.4024	B
142	69.34	1.3541	22.92	12.12	0.3900	C
143	69.34	1.3541	23.02	12.17	0.3900	B

Integrated Profile Areas

Based on calculated profile

Profile area	*Counts*	*Amount*
Overall diffraction profile	320737	100.00%
Background radiation	226191	70.52%
Diffraction peaks	94546	29.48%
Peak area belonging to selected phases	34575	10.78%
Peak area of phase A (Quartz)	*19883*	*6.20%*
Peak area of phase B (Illite)	*14593*	*4.55%*
Peak area of phase C (Pyrite)	*99*	*0.03%*
Unidentified peak area	59971	18.70%

Peak Residuals

Peak data	*Counts*	*Amount*
Overall peak intensity	1967	100.00%
Peak intensity belonging to selected phases	1657	84.26%
Unidentified peak intensity	310	15.74%

Diffraction Pattern Graphics

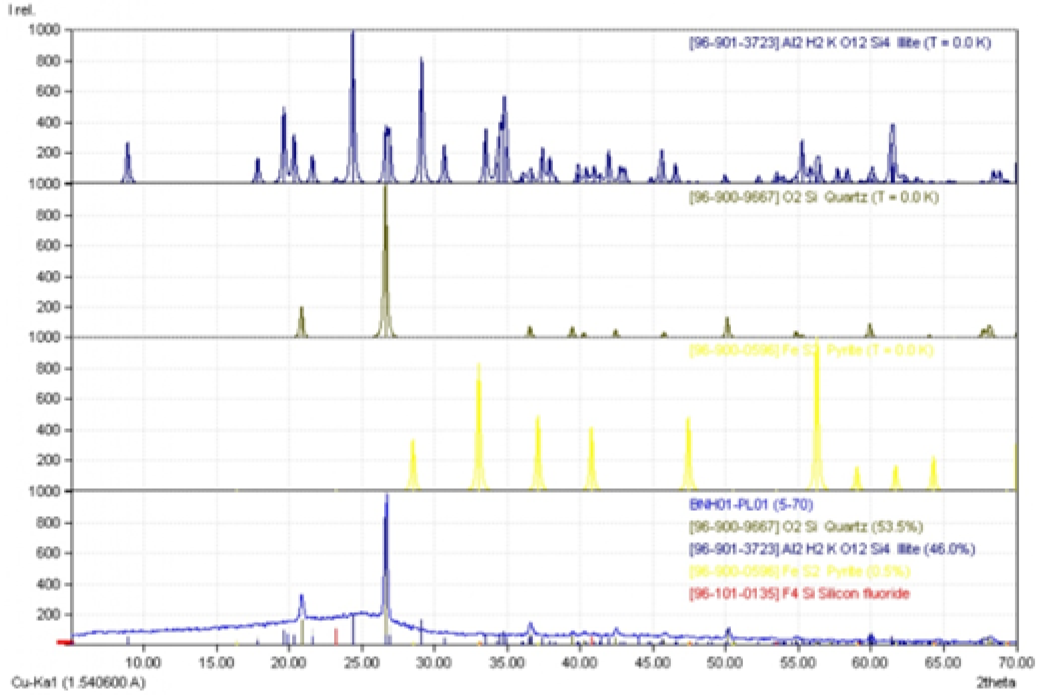
I rel.
[96-901-3723] Al2 H2 K O12 Si4 Illite (T = 0.0 K)
[96-900-9667] O2 Si Quartz (T = 0.0 K)
[96-900-0596] Fe S2 Pyrite (T = 0.0 K)
BNH01-PL01 (5-70)
[96-900-9667] O2 Si Quartz (53.5%)
[96-901-3723] Al2 H2 K O12 Si4 Illite (46.0%)
[96-900-0596] Fe S2 Pyrite (0.5%)
[96-101-0135] F4 Si Silicon fluoride
Cu-Ka1 (1.540600 A)
2theta

Lampiran L. Laporan hasil analisis X-Ray Diffraction (XRD) sampel BNH01_PL02

Match! Phase Analysis Report

Sample: BNH01-PL02 (5-70)

Sample Data

File name	BNH01-PL02.RAW
File path	F:/PASCA SARJANA TAMBANG UNHAS/02. Proposal/02. Analisa/02. Hasil Analisa/05. XRD/XRD BNH/BNH01-PL02
Data collected	Feb 8, 2022 13:15:38
Data range	5.000° - 70.000°
Original data range	5.000° - 70.000°
Number of points	3251
Step size	0.020
Rietveld refinement converged	No
Alpha2 subtracted	No
Background subtr.	No
Data smoothed	Yes
Radiation	X-rays
Wavelength	1.540600 Å

Analysis Results

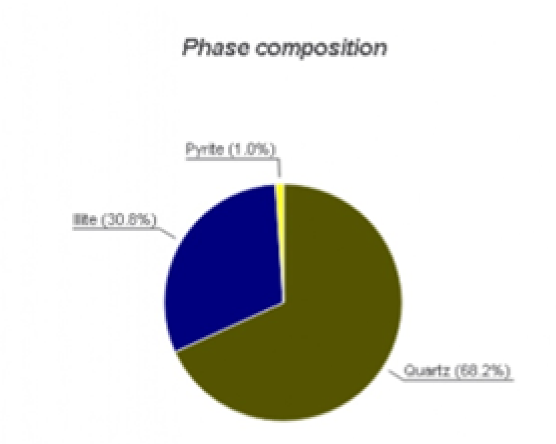

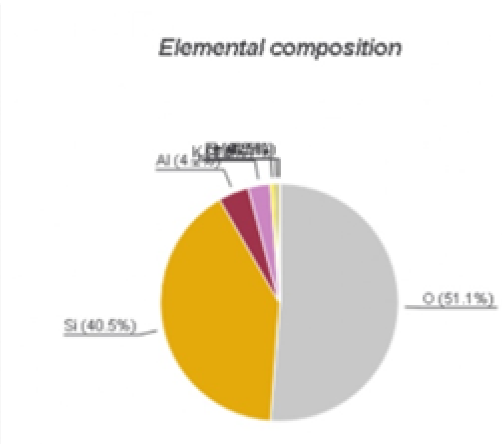

Index	Amount (%)	Name	Formula sum
A	68.2	Quartz	O2 Si
B	30.8	Illite	Al2 H2 K O12 Si4
C	1.0	Pyrite	Fe S2
	18.9	*Unidentified peak area*	

Amounts calculated by RIR (Reference Intensity Ratio) method after manual adjustment of intensity scaling factor(s)

Element	Amount (weight %)
O	51.1%(*)
Si	40.5%
Al	4.2%
K	3.0%
S	0.5%
Fe	0.5%
H	0.2%(*)
*LE (sum)	51.3%

Details of identified phases

A: Quartz (68.2 %)

Formula sum	O2 Si
Entry number	96-900-5018
Figure-of-Merit (FoM)	0.868795
Total number of peaks	70
Peaks in range	18
Peaks matched	18
Intensity scale factor	1.09
Space group	P 32 2 1 S
Crystal system	trigonal (hexagonal axes)
Unit cell	a= 4.9137 Å c= 5.4047 Å
I/Ic	2.96
Calc. density	2.649 g/cm³

Reference	Kihara K., "An X-ray study of the temperature dependence of the quartz structureSample: at T = 298 K", European Journal of Mineralogy **2**, 63-77 (1990)

B: Illite (30.8 %)

Formula sum	Al2 H2 K O12 Si4
Entry number	96-901-3719
Figure-of-Merit (FoM)	0.926643
Total number of peaks	302
Peaks in range	110
Peaks matched	110
Intensity scale factor	0.14
Space group	C 1 2/m 1
Crystal system	monoclinic
Unit cell	a= 5.2021 Å b= 8.9797 Å c= 10.2260 Å β= 101.570 °
I/Ic	0.82
Calc. density	2.834 g/cm³
Reference	Drits V. A., Zviagina B. B., McCarty D. K., Salyn A. L., "Factors responsible for crystal-chemical variations in the solid solutionsfrom illite to aluminoceladonite and from glauconite to celadoniteLocality: Silver caldera, San Juan Mountains, ColoradoSample Name: RM30", American Mineralogist **95**, 348-361 (2010)

C: Pyrite (1.0 %)

Formula sum	Fe S2
Entry number	96-901-5843
Figure-of-Merit (FoM)	0.642209
Total number of peaks	29
Peaks in range	10
Peaks matched	10
Intensity scale factor	0.02
Space group	P a -3
Crystal system	cubic
Unit cell	a= 5.4140 Å
I/Ic	3.29
Calc. density	5.022 g/cm³
Reference	Oftedal I., "Uber die Kristallstrukturen der verbindungen RuS2, OsS2, MnTe2 und AuSb2.Mit einem Anhang uber die Gitterkonstant von Pyrit", Zeitschrift fur Physikalische Chemie **135**, 291-299 (1928)

Candidates

Name	*Formula*	*Entry No.*	*FoM*
Quartz	O2 Si	96-901-5023	0.6812
Si O2	O2 Si	96-153-2513	0.6778
	Li3 Mo3 O12 V	96-400-0872	0.6243
	In5 Mn4 Rb Se12	96-412-0429	0.6203
Genthelvite	Be3 O12 S Si3 Zn4	96-900-0952	0.6109
Titanium tungsten oxide (0.54/0.46/2)	O2 Ti0.54 W0.46	96-200-2762	0.6095
	Cs In5 Mn4 Se12	96-412-0430	0.6068
Quartz	O2 Si	96-900-5019	0.6004
Quartz	O2 Si	96-901-0145	0.5960
Quartz	O2 Si	96-900-5024	0.5850
Quartz	O2 Si	96-900-5021	0.5775
Quartz	O2 Si	96-900-5022	0.5652
Quartz	O2 Si	96-900-5020	0.5643
Quartz	O2 Si	96-901-1494	0.5623
Quartz	O2 Si	96-900-5023	0.5519
chalcopyrite (?Chalkopyrit?)	Cu0.5 Fe0.5 S	96-724-2111	0.0000
Arsenopyrite	As Fe S	96-900-0110	0.0000
Pyrite	Fe S2	96-900-0595	0.0000
Pyrite	Fe S2	96-900-0596	0.0000
Quartz	O2 Si	96-900-0776	0.0000
Quartz	O2 Si	96-900-0777	0.0000
Quartz	O2 Si	96-900-0778	0.0000
Quartz	O2 Si	96-900-0779	0.0000
Quartz	O2 Si	96-900-0780	0.0000
Quartz	O2 Si	96-900-0781	0.0000
Minehillite	Al2 Ca14 H8 K0.948 O64 Si20 Zn2.406	96-900-1665	0.0000
Leadhillite	C2 H2 O12 Pb4 S	96-900-3815	0.0000
Hillite	Ca2 H4 Mg0.377 O10 P2 Zn0.623	96-900-4787	0.0000
Bobtraillite	B3 H18 Na6.462 O78 Si21 Sr5.496 Zr7	96-900-4919	0.0000
Quartz	O2 Si	96-900-5018	0.0000
Quartz	O2 Si	96-900-5025	0.0000
Quartz	O2 Si	96-900-5026	0.0000
Quartz	O2 Si	96-900-5027	0.0000
Quartz	O2 Si	96-900-5028	0.0000
Quartz	O2 Si	96-900-5029	0.0000
Quartz	O2 Si	96-900-5030	0.0000
Quartz	O2 Si	96-900-5031	0.0000

Quartz	O2 Si	96-900-5032	0.0000
Quartz	O2 Si	96-900-5033	0.0000
Quartz	O2 Si	96-900-5034	0.0000
Pyrite	Cu0.25 Fe0.75 S2	96-900-6171	0.0000
Pyrite	Cu0.6 Fe0.4 S2	96-900-6172	0.0000
Quartz	O2 Si	96-900-7379	0.0000
Afwillite	Ca3 H6 O10 Si2	96-900-7429	0.0000
Chalcopyrite	Cu Fe S2	96-900-7573	0.0000
Afwillite	Ca3 H6 O10 Si2	96-900-7612	0.0000
Quartz	O2 Si	96-900-8093	0.0000
Quartz	O2 Si	96-900-8094	0.0000
Kaolinite	Al2 H4 O9 Si2	96-900-9231	0.0000
Kaolinite	Al2 H4 O9 Si2	96-900-9235	0.0000
Tweddillite	Al1.43 Ca Fe0.257 H Mn1.313 O13 Si3 Sr	96-900-9523	0.0000
Illite	Al4 K O12 Si2	96-900-9666	0.0000

and 64 others...

Search-Match

Settings

Reference database used	COD-Inorg 2022.06.29
Automatic zeropoint adaptation	Yes
Downgrade entries with low scaling factors	Yes
Minimum figure-of-merit (FoM)	0.60
2theta window for peak corr.	0.30 deg.
Minimum rel. int. for peak corr.	0
Parameter/influence 2theta	0.50
Parameter/influence intensities	0.50
Parameter multiple/single phase(s)	0.50

Criteria for entries added by user

Reference:

Entry number: 96-101-1098;96-101-1160;96-101-1173;96-101-1177;96-101-1201;96-110-0020;96-500-0036;96-900-0776;96-900-0777;96-900-0778;96-900-0779;96-900-0780;96-900-0781;96-900-5018;96-900-5019;96-900-5020;96-900-5021;96-900-5022;96-900-5023;96-900-5024;96-900-5025;96-900-5026;96-900-5027;96-900-5028;96-900-5029;96-900-5030;96-900-5031;96-900-5032;96-900-5033;96-900-5034;96-900-7379;96-900-8093;96-900-8094;96-900-9667;96-901-0145;96-901-0146;96-901-0147;96-901-1494;96-901-1495;96-901-1496;96-901-1497;96-901-2601;96-901-2602;96-901-2603;96-901-2604;96-901-2605;96-901-2606;96-901-3322;96-901-5023;96-101-0914;96-101-0930;96-101-0941;96-154-4892;96-154-4893;96-154-4894;96-210-4742;96-210-4743;96-210-4753;96-210-4754;96-500-0116;96-724-2111;96-900-0110;96-900-0595;96-900-0596;96-900-6171;96-900-6172;96-900-7573;96-901-0012;96-901-3070;96-901-3071;96-901-3072;96-901-3409;96-901-3698;96-901-5006;96-901-5235;96-901-5637;96-901-5843;96-901-6640;96-101-1046;96-155-0599;96-900-9231;96-900-9235;96-901-5000;96-900-1665;96-900-3815;96-900-4787;96-900-4919;96-900-7429;96-900-7612;96-900-9523;96-900-9666;96-901-0118;96-901-0494;96-901-0549;96-901-1123;96-901-1745;96-901-1746;96-901-2893;96-901-3719;96-901-3720;96-901-3721;96-901-3722;96-901-3723;96-901-3724;96-901-3733;96-901-3985;96-901-4065;96-901-6664

Peak List

No.	***2theta [°]***	***d [Å]***	***I/I0 (peak height)***	***Counts (peak area)***	***FWHM***	***Matched***
1	8.82	10.0182	1.23	3.59	0.9583	B
2	17.69	5.0091	5.03	9.23	0.6010	B
3	19.76	4.4898	7.91	12.74	0.5276	B
4	20.02	4.4323	5.58	9.01	0.5292	B
5	20.43	4.3433	7.48	12.10	0.5300	B
6	20.86	4.2554	190.66	309.07	0.5308	A
7	21.67	4.0972	10.08	15.61	0.5069	B
8	23.30	3.8146	12.90	16.97	0.4306	B
9	24.36	3.6504	19.95	26.42	0.4337	B
10	26.64	3.3434	896.55	657.09	0.2400	A
11	26.64	3.3434	809.76	878.36	0.3552	B
12	26.67	3.3394	1000.00	763.45	0.2500	B
13	28.53	3.1258	7.42	15.48	0.6829	C
14	29.11	3.0647	0.36	0.46	0.4114	B
15	30.55	2.9234	0.74	0.64	0.2800	B
16	33.06	2.7070	9.11	7.68	0.2758	C
17	33.41	2.6795	1.16	0.63	0.1784	B
18	34.51	2.5971	0.23	0.10	0.1400	B
19	34.73	2.5810	0.53	0.23	0.1400	B
20	34.98	2.5631	12.05	5.15	0.1400	B
21	35.19	2.5482	10.44	4.46	0.1400	B
22	35.82	2.5045	0.23	0.10	0.1447	B

23	36.17	2.4812	0.55	0.24	0.1400	B
24	36.37	2.4682	8.98	3.29	0.1200	B
25	36.54	2.4568	42.48	18.16	0.1400	A
26	36.80	2.4402	25.70	6.28	0.0800	B
27	37.10	2.4212	13.89	5.94	0.1400	C
28	37.51	2.3955	1.04	0.53	0.1670	B
29	38.03	2.3643	0.76	0.33	0.1400	B
30	38.12	2.3591	1.70	0.48	0.0927	B
31	39.47	2.2812	30.44	7.44	0.0800	A
32	39.94	2.2557	3.01	1.58	0.1717	B
33	40.08	2.2481	0.80	0.31	0.1259	B
34	40.14	2.2449	4.49	1.69	0.1229	B
35	40.29	2.2366	23.43	8.59	0.1200	A
36	40.68	2.2161	3.56	2.28	0.2103	B
37	40.79	2.2103	6.05	5.56	0.3006	C
38	40.89	2.2050	4.89	3.82	0.2555	B
39	41.18	2.1906	1.16	0.62	0.1752	B
40	41.24	2.1873	1.64	0.64	0.1276	B
41	41.55	2.1716	0.49	0.20	0.1338	B
42	41.98	2.1506	0.38	0.16	0.1369	B
43	42.45	2.1277	22.61	9.66	0.1400	A
44	42.89	2.1068	0.55	0.34	0.2054	B
45	43.29	2.0884	1.23	0.61	0.1627	B
46	44.17	2.0486	3.70	1.58	0.1400	B
47	44.51	2.0338	2.10	3.54	0.5520	B
48	44.94	2.0156	0.73	0.31	0.1400	B
49	45.22	2.0036	2.31	1.06	0.1501	B
50	45.36	1.9977	1.07	0.47	0.1450	B
51	45.79	1.9798	19.22	8.22	0.1400	A
52	46.32	1.9585	0.29	0.51	0.5777	B
53	46.57	1.9486	1.96	2.96	0.4948	B
54	47.46	1.9141	29.95	12.80	0.1400	C
55	47.64	1.9073	6.04	2.49	0.1350	B
56	47.94	1.8962	1.36	0.55	0.1325	B
57	48.84	1.8631	0.36	0.15	0.1400	B
58	49.09	1.8543	1.48	2.30	0.5091	B
59	49.79	1.8297	2.78	1.19	0.1400	B
60	49.93	1.8252	5.19	3.49	0.2200	B
61	50.14	1.8179	49.35	21.10	0.1400	A
62	50.63	1.8016	5.99	13.11	0.7171	A
63	52.06	1.7554	6.47	14.10	0.7131	B
64	53.32	1.7168	2.15	4.69	0.7130	B
65	53.42	1.7139	1.02	2.22	0.7130	B
66	53.46	1.7126	0.76	1.66	0.7130	B
67	53.83	1.7017	1.08	2.33	0.7030	B
68	53.94	1.6984	0.79	1.71	0.7080	B
69	54.10	1.6938	2.25	4.87	0.7105	B
70	54.28	1.6887	0.11	0.24	0.6880	B
71	54.36	1.6864	0.17	0.36	0.6905	B
72	54.43	1.6845	0.60	1.26	0.6905	B
73	54.88	1.6717	22.01	47.92	0.7130	A
74	54.88	1.6717	37.20	15.90	0.1400	B
75	54.95	1.6697	43.02	36.78	0.2800	B
76	54.97	1.6692	42.18	41.22	0.3200	B
77	55.05	1.6668	33.40	24.48	0.2400	B
78	55.13	1.6647	20.94	7.67	0.1200	B
79	55.26	1.6610	4.89	6.22	0.4165	B
80	55.33	1.6590	5.77	12.56	0.7130	A
81	55.58	1.6521	6.44	14.02	0.7130	B
82	56.10	1.6381	0.40	0.88	0.7130	B
83	56.22	1.6349	4.37	9.51	0.7130	B
84	56.31	1.6324	7.61	16.56	0.7130	C
85	56.40	1.6302	8.61	18.74	0.7130	B
86	56.53	1.6268	4.65	10.12	0.7130	B
87	56.54	1.6263	3.53	7.70	0.7130	B
88	57.23	1.6084	5.99	13.04	0.7130	A
89	57.71	1.5963	5.39	8.47	0.5152	B
90	57.91	1.5912	5.53	6.61	0.3912	B
91	58.64	1.5731	5.22	4.26	0.2670	B
92	58.97	1.5650	1.59	0.99	0.2035	B
93	59.06	1.5629	0.85	0.36	0.1400	C
94	59.47	1.5530	0.23	0.10	0.1400	B
95	59.77	1.5459	5.51	2.36	0.1400	B
96	59.96	1.5416	27.52	11.76	0.1400	A
97	60.19	1.5363	2.38	1.02	0.1400	B
98	60.21	1.5356	0.12	0.10	0.2800	B

99	60.36	1.5323	1.66	0.71	0.1400	B
100	61.34	1.5102	0.17	0.07	0.1400	B
101	61.73	1.5016	5.05	2.16	0.1400	C
102	61.80	1.4999	2.56	1.09	0.1400	B
103	61.91	1.4975	1.22	0.52	0.1400	B
104	61.95	1.4966	3.91	1.67	0.1400	B
105	62.04	1.4948	3.50	5.48	0.5133	B
106	62.15	1.4924	0.40	0.40	0.3266	B
107	62.29	1.4893	3.91	2.79	0.2333	B
108	62.72	1.4802	0.08	0.03	0.1400	B
109	62.74	1.4797	0.16	0.23	0.4776	B
110	62.85	1.4774	4.07	3.83	0.3088	B
111	63.12	1.4718	0.29	0.11	0.1244	B
112	63.13	1.4716	0.32	0.12	0.1283	B
113	63.60	1.4617	0.13	0.04	0.1144	B
114	64.04	1.4528	4.71	2.01	0.1400	A
115	64.25	1.4486	6.91	12.95	0.6138	B
116	64.29	1.4478	7.75	7.73	0.3269	B
117	64.33	1.4469	4.85	2.07	0.1400	C
118	64.63	1.4409	3.29	1.41	0.1400	B
119	64.82	1.4372	0.28	0.12	0.1400	B
120	64.98	1.4340	0.64	0.27	0.1400	B
121	65.13	1.4312	3.48	1.49	0.1400	B
122	65.20	1.4297	3.16	1.35	0.1400	B
123	65.27	1.4283	3.19	1.37	0.1400	B
124	65.38	1.4262	2.58	1.10	0.1400	B
125	65.78	1.4185	1.22	0.52	0.1400	A
126	67.43	1.3877	2.01	1.05	0.1562	B
127	67.70	1.3828	52.79	28.24	0.1600	B
128	67.73	1.3824	60.42	32.31	0.1600	B
129	67.74	1.3821	26.77	9.81	0.1200	A
130	68.15	1.3749	58.34	118.19	0.6634	A
131	68.31	1.3720	76.51	65.42	0.2800	A
132	68.31	1.3720	74.49	99.60	0.4000	B
133	68.38	1.3707	74.67	69.89	0.2800	B
134	68.67	1.3657	12.62	11.39	0.2700	B
135	68.79	1.3636	2.06	1.55	0.2250	B
136	68.91	1.3616	1.06	0.86	0.2425	B
137	69.32	1.3544	0.63	0.42	0.2000	B
138	69.38	1.3535	1.46	0.62	0.1400	C

Integrated Profile Areas

Based on calculated profile

Profile area	***Counts***	***Amount***
Overall diffraction profile	200832	100.00%
Background radiation	100227	49.91%
Diffraction peaks	100605	50.09%
Peak area belonging to selected phases	62635	31.19%
Peak area of phase A (Quartz)	*49027*	*24.41%*
Peak area of phase B (Illite)	*12554*	*6.25%*
Peak area of phase C (Pyrite)	*1054*	*0.53%*
Unidentified peak area	37971	18.91%

Peak Residuals

Peak data	***Counts***	***Amount***
Overall peak intensity	3747	100.00%
Peak intensity belonging to selected phases	3262	87.05%
Unidentified peak intensity	485	12.95%

Diffraction Pattern Graphics

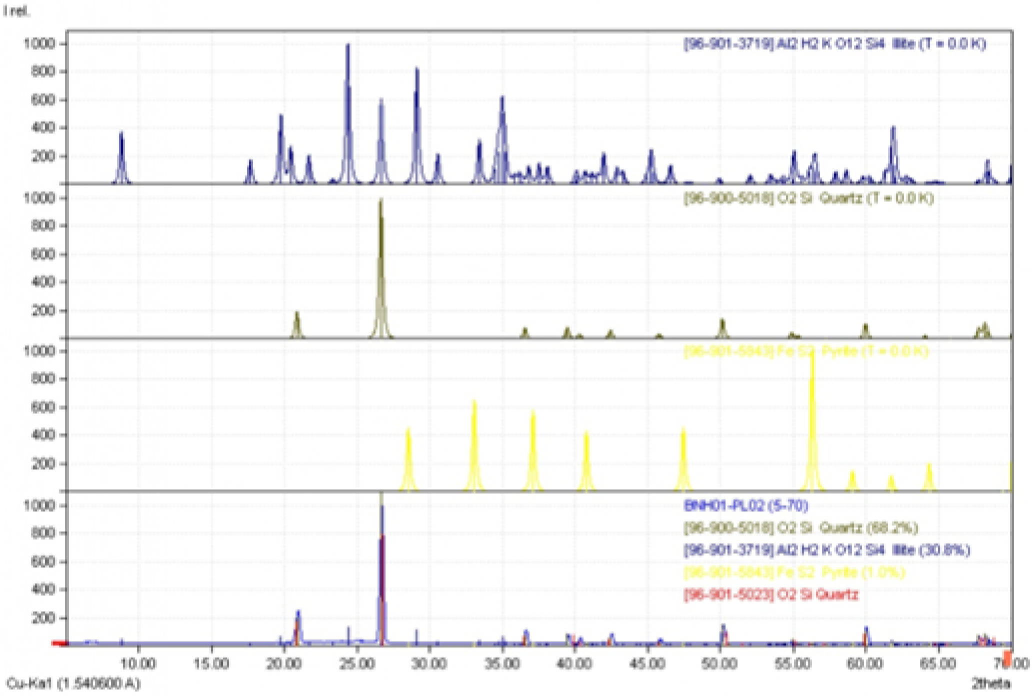
I rel.
[96-901-3719] Al2 H2 K O12 Si4 Illite (T = 0.0 K)
[96-900-5018] O2 Si Quartz (T = 0.0 K)
[96-901-5843] Fe S2 Pyrite (T = 0.0 K)
BNH01-PL02 (5-70)
[96-900-5018] O2 Si Quartz (68.2%)
[96-901-3719] Al2 H2 K O12 Si4 Illite (30.8%)
[96-901-5843] Fe S2 Pyrite (1.0%)
[96-901-5023] O2 Si Quartz
Cu-Ka1 (1.540600 A)
2theta

Lampiran M. Laporan hasil analisis X-Ray Diffraction (XRD) sampel BNH02_PL01

Match! Phase Analysis Report

Sample: BNH02-PL01 (5-70)

Sample Data

File name	BNH02-PL01.RAW
File path	F:/PASCA SARJANA TAMBANG UNHAS/02. Proposal/02. Analisa/02. Hasil Analisa/05. XRD/XRD BNH/BNH02-PL01
Data collected	Feb 8, 2022 13:15:38
Data range	5.000° - 70.000°
Original data range	5.000° - 70.000°
Number of points	3251
Step size	0.020
Rietveld refinement converged	No
Alpha2 subtracted	No
Background subtr.	No
Data smoothed	Yes
Radiation	X-rays
Wavelength	1.540600 Å

Analysis Results

Phase composition

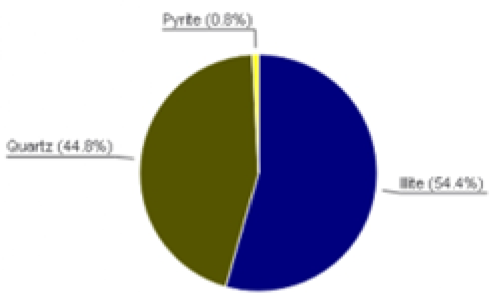

Elemental composition

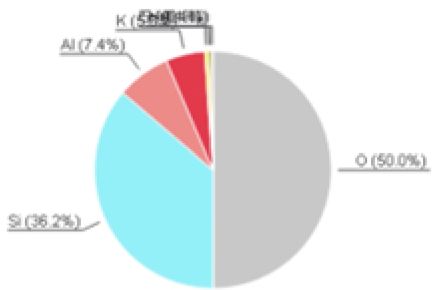

Index	*Amount (%)*	*Name*	*Formula sum*
A	54.4	Illite	Al2 H2 K O12 Si4
B	44.8	Quartz	O2 Si
C	0.8	Pyrite	Fe S2
	18.7	*Unidentified peak area*	

Amounts calculated by RIR (Reference Intensity Ratio) method after manual adjustment of intensity scaling factor(s)

Element	*Amount (weight %)*
O	*50.0%(*)*
Si	36.2%
Al	7.4%
K	5.3%
S	0.4%
Fe	0.4%
H	*0.3%(*)*
**LE (sum)*	*50.3%*

Details of identified phases

A: Illite (54.4 %)

Formula sum	Al2 H2 K O12 Si4
Entry number	96-901-3723
Figure-of-Merit (FoM)	0.943373
Total number of peaks	303
Peaks in range	110
Peaks matched	110
Intensity scale factor	0.32
Space group	C 1 2/m 1
Crystal system	monoclinic
Unit cell	a= 5.2350 Å b= 9.0320 Å c= 10.1400 Å β= 101.520 °
I/Ic	0.79
Calc. density	2.824 g/cm³

Reference	Drits V. A., Zviagina B. B., McCarty D. K., Salyn A. L., "Factors responsible for crystal-chemical variations in the solid solutionsfrom illite to aluminoceladonite and from glauconite to celadoniteLocality: South Urals, RussiaSample Name: 60", American Mineralogist **95**, 348-361 (2010)

B: Quartz (44.8 %)

Formula sum	O2 Si
Entry number	96-900-9667
Figure-of-Merit (FoM)	0.866669
Total number of peaks	71
Peaks in range	18
Peaks matched	18
Intensity scale factor	0.96
Space group	P 31 2 1
Crystal system	trigonal (hexagonal axes)
Unit cell	a= 4.9158 Å c= 5.4091 Å
I/Ic	2.84
Calc. density	2.644 g/cm³
Reference	Gualtieri A. F., "Accuracy of XRPD QPA using the combined Rietveld-RIR methodLocality: Baveno, Novara, Italy", Journal of Applied Crystallography **33**, 267-278 (2000)

C: Pyrite (0.8 %)

Formula sum	Fe S2
Entry number	96-900-0596
Figure-of-Merit (FoM)	0.715874
Total number of peaks	33
Peaks in range	14
Peaks matched	14
Intensity scale factor	0.01
Space group	P 1
Crystal system	triclinic (anorthic)
Unit cell	a= 5.4166 Å b= 5.4166 Å c= 5.4166 Å α= 90.000° β= 90.000 ° γ= 90.000 °
I/Ic	0.99
Calc. density	5.015 g/cm³
Reference	Bayliss P., "Crystal structure refinement of a weakly anisotropic pyrite", American Mineralogist **62**, 1168-1172 (1977)

Candidates

Name	*Formula*	*Entry No.*	*FoM*
Quartz	O2 Si	96-900-5018	0.8023
Quartz	O2 Si	96-901-3322	0.8020
Silicon oxide $-alpha (Quartz low)	O2 Si	96-101-1173	0.8007
Silicon oxide $-alpha (Quartz low)	O2 Si	96-101-1098	0.7989
Silicon oxide (Quartz)	O2 Si	96-500-0036	0.7972
	O2 Si	96-710-3015	0.7911
Quartz	O2 Si	96-900-9667	0.7889
Quartz	O2 Si	96-901-0147	0.7882
	O2 Si	96-230-0371	0.7870
Quartz	O2 Si	96-901-0146	0.7847
	O2 Si	96-210-0189	0.7839
Quartz	O2 Si	96-900-0776	0.7835
Quartz	O2 Si	96-901-2601	0.7825
Quartz	O2 Si	96-900-5019	0.7761
Silicon oxide (Quartz low)	O2 Si	96-101-1160	0.7757
Si O2	O2 Si	96-152-6861	0.7713
Silicon oxide - $-alpha (Quartz low)	O2 Si	96-101-1177	0.7695
Quartz	O2 Si	96-901-0145	0.7666
Quartz	O2 Si	96-901-1494	0.7659
Tridymite	O2 Si	96-901-3394	0.7267
	Be F2	96-153-1932	0.7203
	B N	96-900-8998	0.7187
Berlinite	Al O4 P	96-900-6550	0.7154
Quartz	O2 Si	96-901-5023	0.7123
Se (C N)2	C2 N2 Se	96-153-7589	0.7085
Na0.61 (Co O2)	Co Na0.61 O2	96-153-2938	0.7079
Si O2	O2 Si	96-153-6390	0.7078
Quartz	O2 Si	96-900-5020	0.7011
	Ru	96-153-4915	0.6978
	Rh	96-153-4918	0.6977
(Mn0.3 Rh0.7)	Mn0.3 Rh0.7	96-152-2763	0.6975
Periclase	Mg O	96-901-3271	0.6966
Graphite	C	96-900-8570	0.6949
Graphite	C	96-900-0047	0.6931
Copper-tetracyanoborate	C4 B Cu N4	96-430-8584	0.6916
Lithium	Li	96-901-1566	0.6860
Na0.84 (Co O2)	Co Na0.84 O2	96-153-2991	0.6828

Si O2	O2 Si	96-153-2513	0.6821
Boron Nitride	B N	96-591-0080	0.6797
Quartz	O2 Si	96-900-5021	0.6789
Cadmium iridium hexacyanide dodecahydrate	C12 H24 Cd3 Ir2 N12 O12	96-200-4588	0.6784
Neon	Ne	96-901-1721	0.6778
Silicon fluoride	F4 Si	96-101-0135	0.6753
	Li2 Mg2 Mo3 O12	96-720-4607	0.6732
Al P O4	Al O4 P	96-153-0003	0.6701
Li3 B14	B14 Li3	96-151-1410	0.6694
	C5 Li N O6 P2	96-723-5080	0.6693
Riomarinaite	Bi H3 O6 S	96-901-1238	0.6685
Na0.57 (Co O2)	Co Na0.57 O2	96-153-2940	0.6684
(Fe0.8 Ga0.2)	Fe0.8 Ga0.2	96-152-4161	0.6672
	B15 H60 Li3 Mn Zn5	96-433-8362	0.6668
(Rh0.92 Ta0.08)	Rh0.92 Ta0.08	96-152-3690	0.6664

and 333 others...

Search-Match

Settings

Reference database used	COD-Inorg 2022.06.29
Automatic zeropoint adaptation	Yes
Downgrade entries with low scaling factors	Yes
Minimum figure-of-merit (FoM)	0.60
2theta window for peak corr.	0.30 deg.
Minimum rel. int. for peak corr.	0
Parameter/influence 2theta	0.50
Parameter/influence intensities	0.50
Parameter multiple/single phase(s)	0.50

Criteria for entries added by user

Reference:

Entry number: 96-101-0914;96-101-0930;96-101-0941;96-154-4892;96-154-4893;96-154-4894;96-210-4742;96-210-4743;96-210-4753;96-210-4754;96-500-0116;96-724-2111;96-900-0110;96-900-0595;96-900-0596;96-900-6171;96-900-6172;96-900-7573;96-901-0012;96-901-3070;96-901-3071;96-901-3072;96-901-3409;96-901-3698;96-901-5006;96-901-5235;96-901-5637;96-901-5843;96-901-6640;96-101-1046;96-155-0599;96-900-9231;96-900-9235;96-901-5000;96-101-1098;96-101-1160;96-101-1173;96-101-1177;96-101-1201;96-110-0020;96-500-0036;96-900-0776;96-900-0777;96-900-0778;96-900-0779;96-900-0780;96-900-0781;96-900-5018;96-900-5019;96-900-5020;96-900-5021;96-900-5022;96-900-5023;96-900-5024;96-900-5025;96-900-5026;96-900-5027;96-900-5028;96-900-5029;96-900-5030;96-900-5031;96-900-5032;96-900-5033;96-900-5034;96-900-7379;96-900-8093;96-900-8094;96-900-9667;96-901-0145;96-901-0146;96-901-0147;96-901-1494;96-901-1495;96-901-1496;96-901-1497;96-901-2601;96-901-2602;96-901-2603;96-901-2604;96-901-2605;96-901-2606;96-901-3322;96-901-5023;96-900-1665;96-900-3815;96-900-4787;96-900-4919;96-900-7429;96-900-7612;96-900-9523;96-900-9666;96-901-0118;96-901-0494;96-901-0549;96-901-1123;96-901-1745;96-901-1746;96-901-2893;96-901-3719;96-901-3720;96-901-3721;96-901-3722;96-901-3723;96-901-3724;96-901-3733;96-901-3985;96-901-4065;96-901-6664

Peak List

No.	***2theta [°]***	***d [Å]***	***I/I0 (peak height)***	***Counts (peak area)***	***FWHM***	***Matched***
1	8.89	9.9357	22.09	14.65	1.1880	A
2	16.35	5.4166	146.04	96.87	1.1880	C
3	17.84	4.9679	184.35	97.11	0.9435	A
4	19.64	4.5160	225.34	103.33	0.8213	A
5	19.89	4.4604	217.14	69.93	0.5768	A
6	20.34	4.3620	221.25	63.70	0.5156	A
7	20.85	4.2572	428.65	296.77	1.2400	B
8	21.60	4.1112	261.78	40.93	0.2800	A
9	23.20	3.8301	307.37	36.04	0.2100	C
10	23.22	3.8283	311.31	48.67	0.2800	A
11	24.37	3.6488	341.05	53.32	0.2800	A
12	26.62	3.3453	1000.00	178.67	0.3200	B
13	26.65	3.3417	916.48	163.75	0.3200	A
14	26.90	3.3119	298.22	46.62	0.2800	A
15	28.52	3.1273	98.58	13.21	0.2400	C
16	29.11	3.0649	83.36	28.66	0.6158	A
17	30.68	2.9121	21.62	10.00	0.8278	A
18	33.05	2.7083	98.34	7.69	0.1400	C
19	33.53	2.6707	1.99	0.16	0.1400	A
20	34.29	2.6129	3.51	0.27	0.1400	A
21	34.52	2.5965	20.31	1.59	0.1400	A
22	34.79	2.5766	27.78	2.17	0.1400	A

23	34.96	2.5648	9.55	0.75	0.1400	A
24	36.03	2.4907	14.59	2.36	0.2902	A
25	36.13	2.4839	24.91	1.95	0.1400	A
26	36.46	2.4622	48.59	6.93	0.2556	A
27	36.53	2.4579	71.79	14.88	0.3712	B
28	36.62	2.4522	78.46	11.20	0.2556	A
29	37.08	2.4224	359.91	28.13	0.1400	C
30	37.39	2.4030	4.19	0.33	0.1400	A
31	37.91	2.3714	16.93	1.90	0.2006	A
32	38.26	2.3505	10.17	1.31	0.2308	A
33	39.44	2.2828	49.14	14.39	0.5247	B
34	39.83	2.2616	20.98	6.23	0.5321	A
35	39.89	2.2580	27.51	8.23	0.5358	A
36	39.90	2.2578	27.22	8.17	0.5376	A
37	40.27	2.2377	63.93	18.09	0.5069	B
38	40.41	2.2302	57.21	12.45	0.3899	A
39	40.77	2.2113	44.03	13.99	0.5691	C
40	40.77	2.2112	40.15	11.64	0.5191	A
41	40.96	2.2018	34.76	9.59	0.4941	A
42	41.36	2.1810	40.66	10.08	0.4441	A
43	41.46	2.1764	61.76	10.42	0.3021	A
44	41.95	2.1517	0.82	0.10	0.2184	A
45	42.43	2.1286	1.28	0.10	0.1400	B
46	42.75	2.1134	0.64	0.10	0.2783	A
47	43.05	2.0995	29.80	3.00	0.1400	A
48	44.02	2.0556	17.49	7.12	0.5652	A
49	44.70	2.0257	17.36	7.36	0.5892	A
50	44.85	2.0195	29.65	12.84	0.6012	A
51	45.44	1.9944	17.92	7.77	0.6021	A
52	45.62	1.9871	25.16	10.81	0.5966	A
53	45.77	1.9807	26.94	8.40	0.5584	B
54	46.54	1.9499	12.86	5.12	0.5529	A
55	46.66	1.9450	12.00	4.99	0.5774	A
56	47.44	1.9150	41.15	13.08	0.5691	C
57	47.46	1.9142	30.50	12.50	0.5691	A
58	48.02	1.8930	16.65	6.71	0.5591	A
59	48.77	1.8657	6.35	2.53	0.5541	A
60	49.04	1.8563	20.77	8.14	0.5441	A
61	49.95	1.8244	34.16	13.63	0.5538	A
62	50.11	1.8190	47.62	14.78	0.5560	B
63	50.11	1.8188	37.77	15.19	0.5582	A
64	50.51	1.8055	24.22	7.70	0.5691	C
65	50.58	1.8030	19.25	6.12	0.5691	B
66	52.26	1.7490	12.72	5.22	0.5691	A
67	53.32	1.7169	11.68	4.79	0.5691	A
68	53.45	1.7129	13.03	4.14	0.5691	C
69	53.46	1.7127	10.03	4.71	0.6517	A
70	53.53	1.7106	7.23	3.61	0.6930	A
71	53.60	1.7084	10.12	5.20	0.7137	A
72	53.61	1.7082	10.79	5.47	0.7034	A
73	53.76	1.7038	19.11	10.75	0.7807	A
74	53.95	1.6982	5.08	2.94	0.8038	A
75	54.04	1.6956	10.46	6.14	0.8154	A
76	54.07	1.6948	10.71	6.33	0.8212	A
77	54.58	1.6800	3.44	2.28	0.9216	A
78	54.83	1.6729	14.90	10.31	0.9607	A
79	54.84	1.6727	19.47	10.60	0.9748	B
80	54.91	1.6708	19.46	13.86	0.9889	A
81	55.25	1.6612	5.89	4.09	0.9634	A
82	55.26	1.6611	6.39	4.41	0.9594	A
83	55.29	1.6603	13.89	7.07	0.9115	B
84	55.44	1.6559	14.33	9.60	0.9298	A
85	55.71	1.6486	2.65	1.80	0.9422	A
86	55.82	1.6455	83.90	57.46	0.9509	A
87	56.21	1.6353	8.43	5.77	0.9500	A
88	56.28	1.6332	8.52	4.47	0.9396	C
89	56.29	1.6331	3.56	2.42	0.9448	A
90	56.37	1.6310	3.80	2.57	0.9396	A
91	56.44	1.6291	9.18	6.14	0.9296	A
92	57.20	1.6091	28.01	13.87	0.8871	B
93	57.34	1.6055	9.33	6.02	0.8958	A
94	57.69	1.5966	3.89	2.55	0.9114	A
95	58.36	1.5798	16.14	10.92	0.9398	A
96	59.03	1.5636	17.13	8.99	0.9396	C
97	59.27	1.5577	17.16	11.55	0.9346	A
98	59.40	1.5547	6.30	4.24	0.9346	A

99	59.90	1.5430	25.07	16.79	0.9302	A
100	59.93	1.5423	60.24	31.39	0.9333	B
101	60.08	1.5387	44.15	29.80	0.9372	A
102	60.10	1.5382	40.38	27.27	0.9376	A
103	60.35	1.5324	6.06	4.10	0.9384	A
104	61.38	1.5093	6.94	4.70	0.9394	A
105	61.51	1.5062	4.29	2.91	0.9395	A
106	61.56	1.5053	3.61	2.44	0.9395	A
107	61.60	1.5044	2.14	1.45	0.9396	A
108	61.69	1.5023	1.77	0.93	0.9396	C
109	61.91	1.4976	71.05	47.83	0.9346	A
110	62.04	1.4948	2.63	1.76	0.9321	A
111	62.18	1.4917	1.24	0.83	0.9308	A
112	62.34	1.4883	2.17	1.42	0.9077	A
113	62.41	1.4868	66.90	43.99	0.9130	A
114	62.93	1.4758	58.11	38.24	0.9136	A
115	63.14	1.4713	3.68	2.35	0.8866	A
116	63.45	1.4649	80.39	35.04	0.7807	A
117	63.88	1.4560	25.79	13.24	0.9197	A
118	63.98	1.4540	65.78	43.81	0.9247	A
119	63.99	1.4538	1.83	0.95	0.9321	B
120	64.15	1.4506	18.48	12.46	0.9358	A
121	64.30	1.4476	19.07	10.00	0.9396	C
122	64.65	1.4406	66.77	42.43	0.8825	A
123	64.78	1.4379	48.49	30.22	0.8653	A
124	64.96	1.4344	7.54	4.68	0.8625	A
125	64.99	1.4339	8.37	5.19	0.8611	A
126	65.26	1.4286	1.40	0.85	0.8418	A
127	65.39	1.4260	56.12	33.43	0.8269	A
128	65.73	1.4194	11.67	6.97	0.8285	A
129	65.75	1.4191	13.92	6.45	0.8300	B
130	67.19	1.3921	11.31	6.91	0.8478	A
131	67.52	1.3862	2.12	1.30	0.8481	A
132	67.70	1.3828	36.31	17.19	0.8481	B
133	67.71	1.3827	29.80	18.20	0.8481	A
134	68.10	1.3758	37.06	17.55	0.8481	B
135	68.28	1.3726	64.33	30.46	0.8482	B
136	68.40	1.3704	42.35	25.87	0.8482	A
137	68.42	1.3701	38.31	23.40	0.8482	A
138	68.80	1.3635	2.83	1.73	0.8482	A
139	68.85	1.3625	53.89	32.92	0.8482	A
140	68.94	1.3609	51.09	31.21	0.8482	A
141	69.34	1.3541	5.17	2.45	0.8482	C
142	69.34	1.3541	60.72	35.78	0.8182	A

Integrated Profile Areas

Based on calculated profile

Profile area	***Counts***	***Amount***
Overall diffraction profile	386777	100.00%
Background radiation	284483	73.55%
Diffraction peaks	102294	26.45%
Peak area belonging to selected phases	30083	7.78%
Peak area of phase A (Illite)	*16941*	*4.38%*
Peak area of phase B (Quartz)	*13018*	*3.37%*
Peak area of phase C (Pyrite)	*123*	*0.03%*
Unidentified peak area	72211	18.67%

Peak Residuals

Peak data	***Counts***	***Amount***
Overall peak intensity	2744	100.00%
Peak intensity belonging to selected phases	2136	77.82%
Unidentified peak intensity	609	22.18%

Diffraction Pattern Graphics

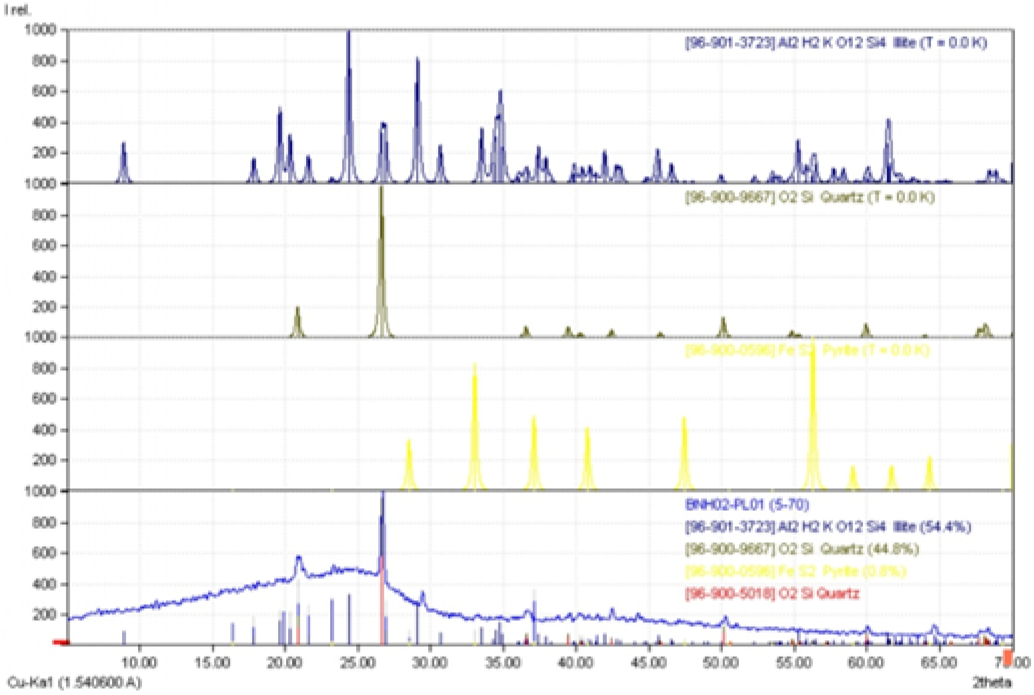

Match! Copyright © 2003-2022 CRYSTAL IMPACT, Bonn, Germany

Lampiran N. Laporan hasil analisis X-Ray Diffraction (XRD) sampel BNH02_PL02

Match! Phase Analysis Report

Sample: BNH02-PL02 (5-70)

Sample Data	
File name	BNH02-PL02.RAW
File path	F:/PASCA SARJANA TAMBANG UNHAS/02. Proposal/02. Analisa/02. Hasil Analisa/05. XRD/XRD BNH/BNH02-PL02
Data collected	Feb 8, 2022 13:15:38
Data range	5.000° - 70.000°
Original data range	5.000° - 70.000°
Number of points	3251
Step size	0.020
Rietveld refinement converged	No
Alpha2 subtracted	No
Background subtr.	No
Data smoothed	Yes
Radiation	X-rays
Wavelength	1.540600 Å

Analysis Results

Phase composition

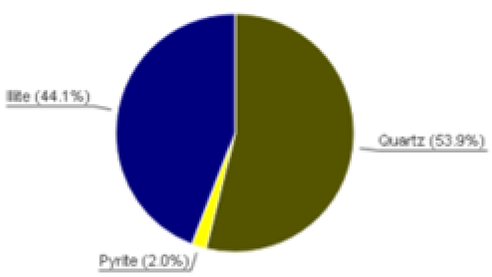

Elemental composition

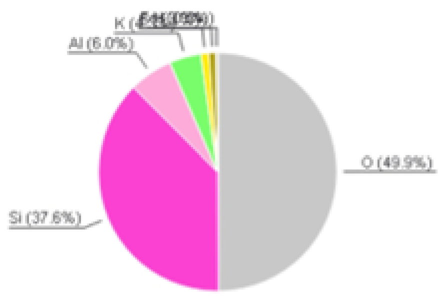

Index	Amount (%)	Name	Formula sum
A	53.9	Quartz	O2 Si
B	2.0	Pyrite	Fe S2
C	44.1	Illite	Al2 H2 K O12 Si4
	38.0	*Unidentified peak area*	

Amounts calculated by RIR (Reference Intensity Ratio) method

Element	Amount (weight %)
O	49.9%(*)
Si	37.6%
Al	6.0%
K	4.3%
S	1.1%
Fe	0.9%
H	0.2%(*)
*LE (sum)	50.1%

Details of identified phases

A: Quartz (53.9 %)	
Formula sum	O2 Si
Entry number	96-901-0145
Figure-of-Merit (FoM)	0.826237
Total number of peaks	72
Peaks in range	18
Peaks matched	15
Intensity scale factor	0.48
Space group	P 32 2 1 S
Crystal system	trigonal (hexagonal axes)
Unit cell	a= 4.9230 Å c= 5.4090 Å
I/Ic	2.86
Calc. density	2.636 g/cm³

Reference	Ikuta D., Kawame N., Banno S., Hirajima T., Ito K., Rakovan J. F., Downs R. T., Tamada O., "First in situ X-ray diffraction identification of coesite and retrogradequartz on a glass thin section of an ultrahigh-pressure metamorphic rock andtheir crystal structure details Locality: Yangkou meta-igneous complex in themiddle part of the Sulu UHP terrain, eastern China Note: Sample is on a thinsection", American Mineralogist **92**, 57-63 (2007)

B: Pyrite (2.0 %)*

Formula sum	Fe S2
Entry number	96-900-0596
Figure-of-Merit (FoM)	0.494051*
Total number of peaks	33
Peaks in range	14
Peaks matched	9
Intensity scale factor	0.01*
Space group	P 1
Crystal system	triclinic (anorthic)
Unit cell	a= 5.4166 Å b= 5.4166 Å c= 5.4166 Å α= 90.000° β= 90.000 ° γ= 90.000 °
I/Ic	0.99
Calc. density	5.015 g/cm³
Reference	Bayliss P., "Crystal structure refinement of a weakly anisotropic pyrite", American Mineralogist **62**, 1168-1172 (1977)

C: Illite (44.1 %)

Formula sum	Al2 H2 K O12 Si4
Entry number	96-901-3733
Figure-of-Merit (FoM)	0.803909
Total number of peaks	303
Peaks in range	110
Peaks matched	83
Intensity scale factor	0.09
Space group	C 1 2 1
Crystal system	monoclinic
Unit cell	a= 5.1973 Å b= 8.9990 Å c= 10.1470 Å β= 99.000 °
I/Ic	0.67
Calc. density	2.830 g/cm³
Reference	Drits V. A., Zviagina B. B., McCarty D. K., Salyn A. L., "Factors responsible for crystal-chemical variations in the solid solutionsfrom illite to aluminoceladonite and from glauconite to celadoniteLocality: Athabasca basement", American Mineralogist **95**, 348-361 (2010)

(*) 2theta values have been shifted internally for the calculation of the amounts, the intensity scaling factors as well as the figure-of-merit (FoM), due to the active search-match option 'Automatic zero point adaption'.

Candidates

Name	*Formula*	*Entry No.*	*FoM*
	Rh Ti	96-152-3125	0.6472
	Nb	96-153-4904	0.6464
La Pd3 B	B La Pd3	96-151-1208	0.6267
(Ga0.4 Re0.6)	Ga0.4 Re0.6	96-152-2718	0.6218
	La Pd3	96-153-8083	0.6195
	La Pd3	96-152-3423	0.6155
chalcopyrite (?Chalkopyrit?)	Cu0.5 Fe0.5 S	96-724-2111	0.0000
Arsenopyrite	As Fe S	96-900-0110	0.0000
Pyrite	Fe S2	96-900-0595	0.0000
Pyrite	Fe S2	96-900-0596	0.0000
Minehillite	Al2 Ca14 H8 K0.948 O64 Si20 Zn2.406	96-900-1665	0.0000
Leadhillite	C2 H2 O12 Pb4 S	96-900-3815	0.0000
Hillite	Ca2 H4 Mg0.377 O10 P2 Zn0.623	96-900-4787	0.0000
Bobtraillite	B3 H18 Na6.462 O78 Si21 Sr5.496 Zr7	96-900-4919	0.0000
Pyrite	Cu0.25 Fe0.75 S2	96-900-6171	0.0000
Pyrite	Cu0.6 Fe0.4 S2	96-900-6172	0.0000
Afwillite	Ca3 H6 O10 Si2	96-900-7429	0.0000
Chalcopyrite	Cu Fe S2	96-900-7573	0.0000
Afwillite	Ca3 H6 O10 Si2	96-900-7612	0.0000
Kaolinite	Al2 H4 O9 Si2	96-900-9231	0.0000
Kaolinite	Al2 H4 O9 Si2	96-900-9235	0.0000
Tweddillite	Al1.43 Ca Fe0.257 H Mn1.313 O13 Si3 Sr	96-900-9523	0.0000
Illite	Al4 K O12 Si2	96-900-9666	0.0000
Pyrite	Fe S2	96-901-0012	0.0000
Merrillite	Ca9 Fe0.2 Mg0.8 Na0.23 O28 P6.24	96-901-0118	0.0000
Merrillite	Ca9.443 Fe0.065 Mg0.935 O28 P6.964	96-901-0494	0.0000
Oneillite	Ca5.31 Ce3.24 Cl2.16 Fe4.28 K La2 Mn11.16 Na41 Nb3 Nd O230.31 Pr0.27 Si75 Y Zr10	96-901-0549	0.0000
Sidwillite	H4 Mo O5	96-901-1123	0.0000
Francevillite	Ba0.96 H10 O17 Pb0.04 U2 V2	96-901-1745	0.0000
Francevillite	Ba0.69 H10 O17 Pb0.31 U2 V2	96-901-1746	0.0000

Amarillite	Fe H12 Na O14 S2	96-901-2893	0.0000
Pyrite	Fe S2	96-901-3070	0.0000
Pyrite	As0.026 Fe S1.974	96-901-3071	0.0000
Pyrite	As0.54 Fe S1.46	96-901-3072	0.0000
Arsenopyrite	As0.91 Co0.13 Fe0.87 S1.09	96-901-3409	0.0000
Argentopyrite	Ag Fe2 S3	96-901-3698	0.0000
Illite	Al2 H2 K O12 Si4	96-901-3719	0.0000
Illite	Al2 H2 K O12 Si4	96-901-3720	0.0000
Illite	Al2 H2 K O12 Si4	96-901-3721	0.0000
Illite	Al2 H2 K O12 Si4	96-901-3722	0.0000
Illite	Al2 H2 K O12 Si4	96-901-3723	0.0000
Illite	Al2 H2 K O12 Si4	96-901-3724	0.0000
Illite	Al2 H2 K O12 Si4	96-901-3733	0.0000
Afwillite	Ca3 H6 O10 Si2	96-901-3985	0.0000
Leadhillite	C2 H2 O12 Pb4 S	96-901-4065	0.0000
Kaolinite	Al2 O9 Si2	96-901-5000	0.0000
Chalcopyrite	Cu0.5 Fe0.5 S	96-901-5006	0.0000
Chalcopyrite	Cu Fe S2	96-901-5235	0.0000
Chalcopyrite	Cu Fe S2	96-901-5637	0.0000
Pyrite	Fe S2	96-901-5843	0.0000
Arsenopyrite	As Fe S	96-901-6640	0.0000
Merrillite	Ca9.45 Fe0.22 Mg0.78 O28 P7	96-901-6664	0.0000

and 15 others...

Search-Match

Settings

Reference database used	COD-Inorg 2022.06.29
Automatic zeropoint adaptation	Yes
Downgrade entries with low scaling factors	Yes
Minimum figure-of-merit (FoM)	0.60
2theta window for peak corr.	0.30 deg.
Minimum rel. int. for peak corr.	12
Parameter/influence 2theta	0.50
Parameter/influence intensities	0.50
Parameter multiple/single phase(s)	0.50

Criteria for entries added by user

Reference:

Entry number: 96-101-0914;96-101-0930;96-101-0941;96-154-4892;96-154-4893;96-154-4894;96-210-4742;96-210-4743;96-210-4753;96-210-4754;96-500-0116;96-724-2111;96-900-0110;96-900-0595;96-900-0596;96-900-6171;96-900-6172;96-900-7573;96-901-0012;96-901-3070;96-901-3071;96-901-3072;96-901-3409;96-901-3698;96-901-5006;96-901-5235;96-901-5637;96-901-5843;96-901-6640;96-101-1046;96-155-0599;96-900-9231;96-900-9235;96-901-5000;96-900-1665;96-900-3815;96-900-4787;96-900-4919;96-900-7429;96-900-7612;96-900-9523;96-900-9666;96-901-0118;96-901-0494;96-901-0549;96-901-1123;96-901-1745;96-901-1746;96-901-2893;96-901-3719;96-901-3720;96-901-3721;96-901-3722;96-901-3723;96-901-3724;96-901-3733;96-901-3985;96-901-4065;96-901-6664

Peak List

No.	***2theta [°]***	***d [Å]***	***I/I0 (peak height)***	***Counts (peak area)***	***FWHM***	***Matched***
1	8.82	10.0221	1.41	0.18	0.0154	C
2	17.68	5.0114	0.29	0.24	0.1000	C
3	19.71	4.4995	6.75	8.08	0.1419	C
4	19.90	4.4589	0.15	0.34	0.2761	C
5	20.66	4.2965	21.84	29.49	0.1600	C
6	20.82	4.2634	122.93	207.46	0.2000	A
7	21.63	4.1048	1.06	3.01	0.3384	C
8	22.89	3.8827	1.94	4.41	0.2692	C
9	24.84	3.5815	1.40	1.61	0.1365	C
10	26.60	3.3483	498.03	420.23	0.1000	A
11	26.60	3.3479	0.12	0.10	0.1000	C
12	26.66	3.3407	1000.00	843.78	0.1000	C
13	28.52	3.1273	0.97	1.79	0.2200	B
14	28.52	3.1268	1.27	1.77	0.1644	C
15	31.17	2.8670	0.31	0.53	0.1988	C
16	33.05	2.7083	1.96	8.77	0.5290	B
17	33.38	2.6822	0.41	2.47	0.7145	C
18	34.61	2.5899	0.86	5.72	0.7922	C
19	34.67	2.5855	0.85	5.05	0.7041	C
20	34.93	2.5667	1.05	5.22	0.5912	C
21	35.07	2.5569	0.43	1.47	0.4053	C
22	35.68	2.5146	0.69	1.64	0.2802	C

23	35.81	2.5055	0.69	1.63	0.2802	C
24	36.47	2.4615	16.14	10.89	0.0800	A
25	36.48	2.4609	14.79	17.47	0.1400	C
26	36.73	2.4449	46.62	143.62	0.3651	C
27	37.08	2.4223	3.23	2.73	0.1000	B
28	37.48	2.3979	0.09	0.12	0.1618	C
29	37.79	2.3786	0.80	2.75	0.4055	C
30	39.42	2.2838	9.02	63.70	0.8371	A
31	40.05	2.2497	2.88	2.43	0.1000	C
32	40.19	2.2418	7.84	6.62	0.1000	C
33	40.22	2.2404	0.06	0.10	0.2000	A
34	40.41	2.2301	0.12	0.08	0.0800	C
35	40.43	2.2294	42.65	71.98	0.2000	C
36	40.77	2.2113	1.55	1.30	0.1000	B
37	40.81	2.2091	0.12	0.10	0.1000	C
38	41.09	2.1951	0.51	0.43	0.1000	C
39	41.95	2.1519	0.25	0.40	0.1900	C
40	42.03	2.1482	0.32	0.58	0.2150	C
41	42.37	2.1317	9.67	6.52	0.0800	A
42	42.41	2.1298	17.95	31.80	0.2100	C
43	42.69	2.1161	23.19	23.48	0.1200	C
44	44.09	2.0524	0.42	0.96	0.2701	C
45	45.20	2.0044	2.72	4.71	0.2054	C
46	45.71	1.9832	5.39	14.08	0.3093	A
47	45.72	1.9830	6.43	15.66	0.2887	C
48	45.97	1.9728	21.26	74.75	0.4166	C
49	46.48	1.9520	0.37	0.72	0.2300	C
50	46.76	1.9413	0.04	0.07	0.2300	C
51	47.44	1.9150	0.68	1.31	0.2300	B
52	48.48	1.8763	0.29	0.57	0.2300	C
53	48.76	1.8661	0.18	0.49	0.3300	C
54	50.07	1.8204	12.56	8.48	0.0800	A
55	50.96	1.7907	0.45	1.33	0.3499	C
56	52.29	1.7480	0.63	1.84	0.3466	C
57	52.76	1.7337	0.30	0.10	0.0400	C
58	53.37	1.7153	1.48	1.75	0.1400	C
59	53.98	1.6972	0.27	0.32	0.1400	C
60	54.27	1.6890	1.72	1.45	0.1000	C
61	54.55	1.6810	0.82	3.77	0.5472	C
62	54.79	1.6742	4.55	36.87	0.9608	A
63	54.83	1.6731	7.63	17.37	0.2700	C
64	55.03	1.6673	23.43	75.12	0.3800	C
65	55.27	1.6606	3.72	5.02	0.1600	A
66	55.28	1.6604	3.60	5.57	0.1833	C
67	55.46	1.6555	3.54	6.88	0.2300	C
68	55.68	1.6494	0.62	0.65	0.1250	C
69	56.00	1.6407	0.36	0.64	0.2100	C
70	56.24	1.6345	0.84	0.71	0.1000	C
71	56.29	1.6331	3.27	2.76	0.1000	B
72	56.87	1.6178	0.12	0.10	0.1000	C
73	57.41	1.6038	3.53	2.68	0.0900	C
74	57.45	1.6028	0.04	0.10	0.2685	C
75	58.20	1.5838	0.29	0.21	0.0863	C
76	58.51	1.5762	0.06	0.10	0.2000	C
77	58.93	1.5659	0.50	0.38	0.0900	C
78	59.03	1.5636	0.56	0.42	0.0900	B
79	59.04	1.5634	0.12	0.09	0.0900	C
80	59.39	1.5551	0.00	0.00	0.1000	C
81	59.74	1.5467	2.40	2.03	0.1000	C
82	59.84	1.5443	7.40	4.35	0.0697	A
83	60.55	1.5278	0.94	2.09	0.2645	C
84	60.69	1.5246	0.22	0.48	0.2571	C
85	61.24	1.5123	0.72	0.75	0.1235	C
86	61.47	1.5072	0.31	0.35	0.1318	C
87	61.69	1.5023	1.22	1.44	0.1400	B
88	61.80	1.5001	0.24	0.42	0.2100	C
89	61.81	1.4998	0.20	0.34	0.2000	C
90	61.86	1.4987	0.05	0.08	0.2000	C
91	62.57	1.4833	0.12	0.17	0.1700	C
92	62.69	1.4808	0.08	0.06	0.1000	C
93	62.99	1.4744	0.77	0.65	0.1000	C
94	63.11	1.4720	0.05	0.10	0.2554	C
95	63.83	1.4571	0.45	0.64	0.1700	C
96	63.96	1.4545	1.84	2.87	0.1850	A
97	64.30	1.4476	3.63	5.42	0.1770	B
98	64.63	1.4409	0.06	0.14	0.2800	C

99	65.01	1.4335	0.46	1.62	0.4150	C
100	65.68	1.4205	0.27	0.45	0.2000	C
101	65.87	1.4167	0.42	0.70	0.2000	C
102	66.82	1.3990	0.12	0.10	0.1000	C
103	67.62	1.3843	3.80	17.80	0.5550	A
104	68.05	1.3766	19.74	133.25	0.8000	A
105	68.17	1.3745	26.44	198.55	0.8900	A
106	68.75	1.3643	1.63	2.34	0.1700	C
107	69.24	1.3558	0.24	0.20	0.1000	C

Integrated Profile Areas

Based on calculated profile

Profile area	*Counts*	*Amount*
Overall diffraction profile	210919	100.00%
Background radiation	80913	38.36%
Diffraction peaks	130007	61.64%
Peak area belonging to selected phases	49909	23.66%
Peak area of phase A (Quartz)	*33510*	*15.89%*
Peak area of phase B (Pyrite)	*498*	*0.24%*
Peak area of phase C (Illite)	*15901*	*7.54%*
Unidentified peak area	80098	37.98%

Peak Residuals

Peak data	*Counts*	*Amount*
Overall peak intensity	2608	100.00%
Peak intensity belonging to selected phases	2353	90.22%
Unidentified peak intensity	255	9.78%

Diffraction Pattern Graphics

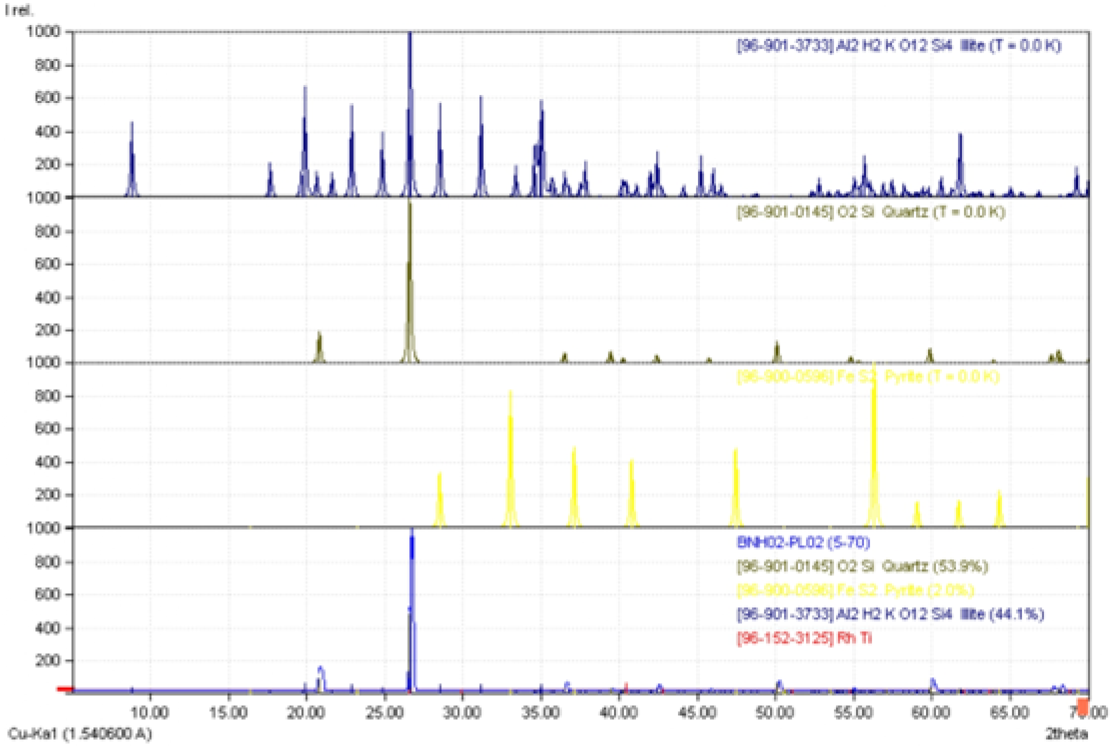

Lampiran O. Hasil Analisis Petrografi Maseral dan Reflectance Vitrinite

F-LP-413.3 Rev.1

KEMENTERIAN ENERGI DAN SUMBER DAYA MINERAL REPUBLIK INDONESIA
BADAN PENELITIAN DAN PENGEMBANGAN ENERGI DAN SUMBER DAYA MINERAL
PUSAT PENELITIAN DAN PENGEMBANGAN TEKNOLOGI MINERAL DAN BATUBARA

Jl. Jenderal Sudirman 623 Bandung – 40211

Tromol Pos : 816 Telepon : (022) 6030483 Fax : (022) 6003373 e-mail : lab_uji@tekmira.esdm.go.id

Nomor: 0954/LBB/XI/2021 30 November 2021

SERTIFIKAT ANALISIS
CERTIFICATE OF ANALYSIS

Dibuat untuk *Certified for*	: Tri Utomo Taliding
Jenis contoh *Type of sample*	: Batubara
Sifat / Kondisi Barang yang diuji *Description of sample*	: -
Asal contoh *Origin of sample*	: Kec. Bonehau, Kab. Mamuju, Provinsi Sulawesi Barat
Jumlah contoh Amount of sample	: 4 (empat)
Nomor laboratorium Laboratory number	: 4279-4282/2021
Contoh diterima Sample received on	: 22 November 2021
Tanggal Selesai Analisis *Date of analysis*	: 30 November 2021
Hasil analisis *Analysis results*	: Hasil Analisis Terlampir

a.n. Kepala Badan Layanan Umum
Pusbitbang tekMIRA
Kepala Bagian Umum,

Agung Surya Dharma.
NIP. 19841017 200901 1 003

1 dari 9

Catatan : 1. Hasil pengujian/analisis ini hanya berlaku untuk contoh yang diuji
Notes: The analysis result are valid only for the tested samples

2. Sertifikat ini tidak boleh diperbanyak (digandakan) tanpa izin dari koordinator teknis
The certificate cannot be reproduced without a written permission from the Technical Coordinator

Tanggal Penerbit/Revisi : 20-04-2018/06-04-2020

MACERAL ANALYSIS

Sample number : 4280/2021
Sample mark : BNHO1-PLO 1

MACERAL ANALYSIS						
MCSERAL	% VOL	VOL (mfb)	SUB MACERAL	MACERAL	% VOL	VOL (mfb)
VITRINITE (HUMINITE)	99.0		Telovitrinite 34.4	Textinite	-	
				Texto-ulminite	-	
				E-ulminite	-	
				Telocollinite	34.4	
			Detrovitrinite (Humodetrinite) 64.6	Attrinite	-	
				Densinite	-	
				Desmocollinite	64.6	
			Gelovitrinite (Humocolinite) -	Corpogelinite	-	
				Porigelinite	-	
				Eugelinite	-	
LIPTINITE (EXINITE)	-			Sporinite	-	
				Cutinite	-	
				Resinite	-	
				Liptodetrinite	-	
				Alginite	-	
				Suberinite	-	
				Fluorinite	-	
				Exsudatinite	-	
				Bituminite	-	
INERTINITE	1.0		Telo-inertinite	Fusinite	-	
				Semifusinite	-	
				Sclerotinite	1.0	
			Detro-inertinite	Inertodetrinite	-	
				Micrinite	-	
			Gelo-inertinite	Macrinite	-	
MINERALS MATTER	-			Oksida	-	
				Pyrite	-	
				Clay	-	
TOTAL	100					

Point Counting : 500 Interval (x) : 2
Magnification : 200x Interval (y) : 2

Prepared and measured in accordance with Australian Standard 2856 (1986) and ASTM (2009)

h

VITRINITE REFLECTANCE ANALYSIS

Sample numbar	: 4280/2021
Sample mark	: BNHO1-PLO 1

Standard Deviation of Sample	: 0.03
Maximum Value (%)	: 0.73
Minimum Value (%)	: 0.64
Mean Maximun Reflectance	: 0.67

Prepared and measured in accordance with Australian Standard 2856 (1986) and ASTM (2009)

MACERAL ANALYSIS

Sample number : 4282/2021
Sample mark : BNHO1-PLO 2

MACERAL ANALYSIS						
MCSERAL	% VOL	VOL (mfb)	SUB MACERAL	MACERAL	% VOL	VOL (mfb)
VITRINITE (HUMINITE)	98.4		Telovitrinite 39.0	Textinite	-	
				Texto-ulminite	-	
				E-ulminite	-	
				Telocollinite	39.0	
			Detrovitrinite (Humodetrinite) 59.4	Attrinite	-	
				Densinite	-	
				Desmocollinite	59.4	
			Gelovitrinite (Humocolinite) -	Corpogelinite	-	
				Porigelinite	-	
				Eugelinite	-	
LIPTINITE (EXINITE)	-			Sporinite	-	
				Cutinite	-	
				Resinite	-	
				Liptodetrinite	-	
				Alginite	-	
				Suberinite	-	
				Fluorinite	-	
				Exsudatinite	-	
				Bituminite	-	
INERTINITE	1.6		Telo-inertinite	Fusinite	-	
				Semifusinite	0.6	
				Sclerotinite	1.0	
			Detro-inertinite	Inertodetrinite	-	
				Micrinite	-	
			Gelo-inertinite	Macrinite	-	
MINERALS MATTER	-			Oksida	-	
				Pyrite	-	
				Clay	-	
TOTAL	100					

Point Counting : 500 Interval (x) : 2
Magnification : 200x Interval (y) : 2

Prepared and measured in accordance with Australian Standard 2856 (1986) and ASTM (2009)

8 dari 9

Catatan : 1. Hasil pengujian/analisis ini hanya berlaku untuk contoh yang diuji
Notes The analysis result are valid only for the tested samples

2. Sertifikat ini tidak boleh diperbanyak (digandakan) tanpa izin dari Koordinator Teknis
The certificate cannot be reproduced without a written permission from the Technical Coordinator

Tanggal Penerbitan/Revisi : 20-04-2018/06-04-2020

VITRINITE REFLECTANCE ANALYSIS

Sample numbar	: 4282/2021
Sample mark	: BNHO1-PLO 2

Standard Deviation of Sample	: 0.02
Maximum Value (%)	: 0.51
Minimum Value (%)	: 0.43
Mean Maximun Reflectance	: 0.47

Prepared and measured in accordance with Australian Standard 2856 (1986) and ASTM (2009)

Laboratorium Batubara,

Astuti Rahayu S.Si
NIP. 19730923 199403 2 002

MACERAL ANALYSIS

Sample number : 4279/2021
Sample mark : BNHO2-PLO 1

MACERAL ANALYSIS						
MCSERAL	% VOL	VOL (mfb)	SUB MACERAL	MACERAL	% VOL	VOL (mfb)
VITRINITE (HUMINITE)	97.2		Telovitrinite 48.6	Textinite	-	
				Texto-ulminite	-	
				E-ulminite	-	
				Telocollinite	48.6	
			Detrovitrinite (Humodetrinite) 48.6	Attrinite	-	
				Densinite	-	
				Desmocollinite	48.6	
			Gelovitrinite (Humocolinite) -	Corpogelinite	-	
				Porigelinite	-	
				Eugelinite	-	
LIPTINITE (EXINITE)	-			Sporinite	-	
				Cutinite	-	
				Resinite	-	
				Liptodetrinite	-	
				Alginite	-	
				Suberinite	-	
				Fluorinite	-	
				Exsudatinite	-	
				Bituminite	-	
INERTINITE	2.8		Telo-inertinite	Fusinite	-	
				Semifusinite	0.6	
				Sclerotinite	2.2	
			Detro-inertinite	Inertodetrinite	-	
				Micrinite	-	
			Gelo-inertinite	Macrinite	-	
MINERALS MATTER				Oksida	-	
				Pyrite	-	
				Clay	-	
TOTAL	100					

Point Counting : 500 Interval (x) : 2
Magnification : 200x Interval (y) : 2

Prepared and measured in accordance with Australian Standard 2856 (1986) and ASTM (2009)

F-LP- 413.3 Rev.1

VITRINITE REFLECTANCE ANALYSIS

Sample numbar	: 4279/2021
Sample mark	: BNHO2-PLO 1

Standard Deviation of Sample	: 0.02
Maximum Value (%)	: 0.68
Minimum Value (%)	: 0.61
Mean Maximun Reflectance	: 0.65

Prepared and measured in accordance with Australian Standard 2856 (1986) and ASTM (2009)

3 dari 9

Catatan : 1. Hasil pengujian/analisis ini hanya berlaku untuk contoh yang diuji
Notes The analysis result are valid only for the tested samples

2. Sertifikat ini tidak boleh diperbanyak (digandakan) tanpa izin dari Koordinator Teknis
The certificate cannot be reproduced without a written permission from the Technical Coordinator

Tanggal Penerbitan/Revisi : 20-04-2018/06-04-2020

MACERAL ANALYSIS

Sample number : 4281/2021
Sample mark : BNHO2-PLO 2

MCSERAL	% VOL	VOL (mfb)	SUB MACERAL	MACERAL	% VOL	VOL (mfb)
VITRINITE (HUMINITE)	95.4		Telovitrinite 41.0	Textinite	-	
				Texto-ulminite	-	
				E-ulminite	-	
				Telocollinite	41.0	
			Detrovitrinite (Humodetrinite) 54.4	Attrinite	-	
				Densinite	-	
				Desmocollinite	54.4	
			Gelovitrinite (Humocolinite) -	Corpogelinite	-	
				Porigelinite	-	
				Eugelinite	-	
LIPTINITE (EXINITE)	-			Sporinite	-	
				Cutinite	-	
				Resinite	-	
				Liptodetrinite	-	
				Alginite	-	
				Suberinite	-	
				Fluorinite	-	
				Exsudatinite	-	
				Bituminite	-	
INERTINITE	3.6		Telo-inertinite	Fusinite	-	
				Semifusinite	-	
				Sclerotinite	3.6	
			Detro-inertinite	Inertodetrinite	-	
				Micrinite	-	
			Gelo-inertinite	Macrinite	-	
MINERALS MATTER	1.0			Oksida	-	
				Pyrite	1.0	
				Clay	-	
TOTAL	100					

Point Counting : 500 Interval (x) : 2
Magnification : 200x Interval (y) : 2

Prepared and measured in accordance with Australian Standard 2856 (1986) and ASTM (2009)

Catatan : 1. Hasil pengujian/analisis ini hanya berlaku untuk contoh yang diuji
Notes The analysis result are valid only for the tested samples

2. Sertifikat ini tidak boleh diperbanyak (digandakan) tanpa izin dari Koordinator Teknis
The certificate cannot be reproduced without a written permission from the Technical Coordinator

Tanggal Penerbitan/Revisi : 20-04-2018/06-04-2020

VITRINITE REFLECTANCE ANALYSIS

Sample numbar	: 4281/2021
Sample mark	: BNHO2-PLO 2

Standard Deviation of Sample	: 0.02
Maximum Value (%)	: 0.51
Minimum Value (%)	: 0.43
Mean Maximun Reflectance	: 0.46

Prepared and measured in accordance with Australian Standard 2856 (1986) and ASTM (2009)

Lampiran P. Hasil Perhitungan TPI dan GI

5. TPI dan GI Sampel BNH01_PL01

- $TPI = \frac{(Telovitrinite + telo{-}inertinite)}{(Detro{-} + gelovitrinite + detro{-} + gelo{-}inertinite)}$

$TPI = \frac{(34,4 + 1)}{(64,6 + 0 + 0 + 0)}$

$TPI = \frac{35,4}{64,6}$

$TPI = 0,55$

- $GI = \frac{(Vitrinite + gelo{-}inertinite)}{(Telo{-}inertinite + detro{-}inertinite)}$

$GI = \frac{(99 + 0)}{(1 + 0)}$

$GI = \frac{99}{1}$

$GI = 99$

6. TPI dan GI Sampel BNH01_PL02

- $TPI = \frac{(Telovitrinite + telo{-}inertinite)}{(Detro{-} + gelovitrinite + detro{-} + gelo{-}inertinite)}$

$TPI = \frac{(39 + 1,6)}{(59,4 + 0 + 0 + 0)}$

$TPI = \frac{40,6}{59,4}$

$TPI = 0,68$

- $GI = \frac{(Vitrinite + gelo{-}inertinite)}{(Telo{-}inertinite + detro{-}inertinite)}$

$GI = \frac{(98,4 + 0)}{(1,6 + 0)}$

$GI = \frac{98,4}{1,6}$

$GI = 61,50$

7. TPI dan GI Sampel BNH02_PL01

- $$TPI = \frac{(Telovitrinite + telo{-}inertinite)}{(Detro{-} + gelovitrinite + detro{-} + gelo{-}inertinite)}$$

  $$TPI = \frac{(48,6 + 2,8)}{(48,6 + 0 + 0 + 0)}$$

  $$TPI = \frac{52,4}{48,6}$$

  $$TPI = 1,06$$

- $$GI = \frac{(Vitrinite + gelo{-}inertinite)}{(Telo{-}inertinite + detro{-}inertinite)}$$

  $$GI = \frac{(97,2 + 0)}{(2,8 + 0)}$$

  $$GI = \frac{97,2}{2,8}$$

  $$GI = 34,71$$

8. TPI dan GI Sampel BNH02_PL02

- $$TPI = \frac{(Telovitrinite + telo{-}inertinite)}{(Detro{-} + gelovitrinite + detro{-} + gelo{-}inertinite)}$$

  $$TPI = \frac{(41 + 3,6)}{(54,4 + 0 + 0 + 0)}$$

  $$TPI = \frac{44,6}{54,4}$$

  $$TPI = 0,82$$

- $$GI = \frac{(Vitrinite + gelo{-}inertinite)}{(Telo{-}inertinite + detro{-}inertinite)}$$

  $$GI = \frac{(95,4 + 0)}{(3,6 + 0)}$$

  $$GI = \frac{95,4}{3,6}$$

  $$GI = 26,50$$

Lampiran Q. Daftar Istilah

Istilah	Arti dan Penjelasan
Adventitious Moisture	Terdiri dari air tanah, yang dimana kelembapan tersebut muncul karena proses yang tidak disengaja
Alluvial Valley	Lembah aluvial Daerah endapan terjadi di sungai, danau yang berada di dataran rendah, ataupun cekungan yang memungkin kan terjadinya endapan, jenis tanah yang terbentuk karena endapan,
Analisis Petrografi	Satu metode visual untuk menggambarkan komposisi dan klasifikasi mineral dari sampel batuan
Anisotropik	Kata benda atau kata sifat untuk menggambarkan materi, mineral, atau proses yang memiliki sifat berbeda di segala arah
Anoxic	Area air laut, air tawar, atau air tanah yang kehabisan oksigen terlarut dan merupakan kondisi hipoksia, Survei geologi as mendefinisikan air tanah anoksik sebagai air dengan konsentrasi oksigen terlarut kurang dari 0,5 miligram per liter
Antiklin	lapisan yang membentuk dua sisi kemiringan berlawanan arah (seakan-akan mempunyai kemiringan yang berlawanan) sama seperti atap rumah,
Antrasit	Batubara keras dengan peringkat teretinggi berwarna hitam dengan kilap tinggi, mengandung persentasi tinggi karbon tertambat (karbon tetap) biasanya antara 92-98% (dalam basis kering, bebas bahan mineral/DMMF),

Ash	Sisa pembakaran dari mineral-mineral yang tidak hangus dalam batubara seperti lempung, kuarsa, pasir, lanau dan belerang bila batubara dibakar, Mineral-mineral tersebut secra kimia dan fisika sama dengan lempung, kuarsa, pasir, lanau, dan belerang yang terdapat di alam,
Banded Coals	Pelapisan batubara yang heterogen, terdiri dari jenis-jenis yang kilapnya berbeda, Banded coal biasanya merupakan batubara bitumen walaupun umumnya batubara dari semua peringkat mempunyai bentuk-bentuk pelapisan,
Bituminous	Jenis batu bara yang menurut klasifikasi ASTM berada diantara antrasit dan batu bara sub bituminus, Batubara yang berada dalam rank bituminous ini memiliki persentase fixed carbon sekitar <69% hingga <86%, Juga, kandungan volatile matter dalam batubara adalah sekitar >32% hingga <22%,
Bog	Bog, merupakan rawa yang banyak ditumbuhi oleh tanaman lumut atau tanaman miskin nutrisi,
Bright Coal	Batubara yang mengkilap, hitam mengkilap menyerupai kilap kaca, atau batubaba yang tidak kusam
Cavities Coal	Rognggа dalam batubara, tempat dimana masuknya mineral yang tidak diinginkan

Channel Sampling	Conto yang diambil dari lapisan batubara dengan membuat torehan memanjang menurut ketebalan batubara atau endapan bahan galian lainnya, Conto ini biasanya diambil sekitar singkapan, Sebelum melakukan pencontoan sumuran atau parit memanjang dibuat untuk membuka satu sisi batubara yang segar,
Charcoal	Arang, Tumbuhan yang sudah terbakar
Cleat	Kekar yakni retakan atau rangkaian hasil gerakan yang merupakan garis atau sisi pemecahan batubara akibat oksidasi atau pelapukan, Biasanya dimanfaatkan menentukan arah penambangan batubara sehingga mudah pemecahannya atau penggaliannya langsung oleh alat muat,
Coal	Batubara dalam istilah yang luas untuk keseluruhan bahan bersifat karbon yang terjadi secara alamiah, Batubara dapat pula didefinisikan sebagai batuan bersifat karbon berbentuk padat, rapuh, berwarna coklat tua sampai hitam,, dapat terbakar, yang terjadi akibat perubahan/pelapukan tumbuhan secara kimia dan fisik,
Coalification	Karbonifikasi berarti proses pengubahan bahan-bahan tambahan pembentuk gambut menjadi lignit kemudian menjadi batubara akibat pengaruh suhu dan tekanan dalam waktu geologis yang lama serta dalam keadaan sedikit sekali udara selama proses berlangsung,

Dekomposisi	Salah satu perubahan secara kimia yang membuat objek, biasanya makhluk hidup yang mati dapat mengalami perusakan susunan/struktur
Dip	Sudut kemiringan lapisan tanah atau batuan ataupun sudut yang dibentuk oleh bidang pelapisan batuan dengan bidang datar yang dinyatakan umumnya dalam derajat
Dull Coals	Komponen lapisan batubara dengan warna keabu-abuan dan tampilan kusam
Eosen	Suatu kala pada skala waktu geologi yang berlangsung 55,8 ± 0,2 hingga 33,9 ± 0,1 juta tahun yang lalu yang merupakan kala kedua pada periode Paleogen di era Kenozoikum
Extraneous *Mineral matter*	Material pembentuk abu yang berasal di luar dari tumbuh-tumbuhan asal batubara,
Fen	Fenogeni, rawa yang banyak ditumbuhi tumbuhan perdu dan beberapa jenis pohon lainnya, Lingkungan ini terkadang basah dan terkadang kering,
Fixed Carbon	Sisa padatan selain dari abu setelah kelengasan dan zat terbang dikeluarkan dari batubara,
Floor	Lapisan bagian paling bawah dari batu bara
Fluorescent	Terpancarnya sinar oleh suatu zat yang telah menyerap sinar atau radiasi elektromagnet lain, Fluoresensi adalah bentuk dari luminesensi, Dalam beberapa hal, sinar yang dipancarkan memiliki gelombang lebih panjang dan energi lebih rendah daripada radiasi yang diserap
Fluvial	Proses yang terkait dengan sungai dan aliran serta endapan dan bentang alam yang dihasilkan,

Fotomikrograf	Foto atau gambar digital yang diambil melalui mikroskop atau perangkat serupa untuk menunjukkan gambar yang diperbesar dari suatu objek,
Fracture	Rekahan pada batubara (cleats) dapat juga berisi gas bebas atau gas yang tersaturasi oleh air
Fusinification	Komponen yang mengalami oksidasi
Gambut	Bahan seperti tanah rawa yang terbentuk terutama dari tumbuhan yang melapuk berwarna kekuning-kuningan sampai hitam kecoklat-coklatan, Dapat juga disebut sebagai endapan tumbuh-tumbuhan yang membusuk tidak sempurna terkumpul di dalam air yang tidak mengalir,
Gelification Index	Merupakan perbandingan antara maseral yang terbentuk akibat proses gelifikasi dan maseral yang terbentuk karena proses oksidasi yang berhubungan dengan kontinuitas kelembapan pada suatu lahan gambut,
Geokimia	Sains yang menggunakan prinsip dan teknologi bidang kimia untuk menganalisis dan menjelaskan mekanisme di balik sistem geologi seperti kerak bumi dan lautan yang berada di atasnya,
Geomorfologi	Sebuah ilmu yang mempelajari tentang bentuk alam dan proses yang membentuknya
Humic Coal	Batubara yang terbentuk dari tumbuhan tingkat tinggi (memiliki akar, batang, dan daun)

Inertinite	Kelompok maseral batu bara yang bila dibakar bersifat lembamn (inert) ; artinya, hampir atau tidak menampakkan sifat plastisitas atau hanya menunjukkan sedikit kecenderungan aglutinasi/melekat selama pengkokasan; terdiri atas makrinit, mikrinit, semifusinit, fusinit, dan sklerotinit
Isotropik	Sifat dan kata benda yang digunakan untuk menggambarkan segala bahan, mineral, atau proses yang memiliki sifat serupa di semua arah
Lignit	Jenis batu bara yang menurut klasifikasi ASTM tergolong ke dalam batu bara termuda yang merupakan tingkat pertama hasil proses pembatu baraan gambut,
Limnic	Merupakan lingkungan dimana batubara terbentuk di bawah air rawa danau
Limno-Telmatic	Lingkungan rawa yang selalu digenangi air, baik saat musim pasang surut ataupun dalam kondisi biasa, Sifat dari rawa ini berupa mesotrofik mengandung percampuran antara air laut dengan air tawar,
Liptinite	Liptinit tidak berasal dari materi yang dapat terhumifikasikan melainkan berasal dari sisa tumbuhan atau dari dari jenis tanaman tingkat rendah sepertispora, ganggang (algae), kutikula, getah tanaman (resin) dan serbuk sari(pollen),
Lower Delta Plain	Sublingkungan ini terletak pada interaksi antara sungai dan laut yang terbentang mulai dari batas surutnya muka air laut yang paling rendah hingga batas maksimal air laut pada saat pasang,

Marsh	Rawa yang banyak ditumbuhi tumbuhan perdu dan jenis tanaman merambat yang umum disekitar danau atau laut
Maseral	Bahan-bahan organik pembentuk batubara, materialnya sangat kecil tidak dapat dilihat langsung, hanya dapat diamati di bawah mikroskop
Metaantrasit	Super antrisit atau antrasit super, yaitu batubara antrasit yang berperingkat tertinggi, mengandung karbon tetap 98% atau lebih, Super antrasit sama dengan meta-antrasit
Mikroskopis	Analisis yang dilakukan dalam studi mineralogi untuk mengamati mineral-mineral yang terkandung dalam bijih atau batubara yang tidak dapat dilihat secara langsung karena bentuknya kecil dan halus,
Mineragrafi	Pengujian mineral bijih dengan mikroskop sinar pantul, merupakan teknik dasar dari mineralogi
Mineral matter	Bahan mineral dalam batubara yang terbenuk pada batubara sejak proses pembentukan batubara, Bahan mineral ini terbawa bersama sisa-sisa tumbuhan pembentukbatubara yang mengandung zat besi, fosfor, belerang, kalsium dan magnesium, Dan juga termasuk bahan anorganik padat didalam batubara,
Miosen	Suatu kala pada skala waktu geologi yang berlangsung antara 23,03 hingga 5,332 juta tahun yang lalu

Nilai Kalori	Tenaga panas dalam satuan kalori, yaitu umlah panas yang dihasilkan (dibebaskan) bila satu unit (satuan) berat atau unit isi bahan bakar dibakar habis (lihat kalori),
Overburden	Lapisan tanah (batuan) yang menutupi lapisan batubara bagian atas, Sering disingkat dengan O/B,Bila Over Burden telah digali diangkat dan dibuang disebut waste (limbah),
Ply	Lapisan tipis batubara baik lapisan tunggal maupun lapisan-lapisan yang dipisahkan oleh batuan antara atau parting ataupun karakter batubara, Dan juga uraian tentang jenis-jenis batuan termasuk batubara sesuai urutan mulai dari lapisan paling atas sampai didasar dari conto inti inti pemboran untuk tujuan analisa lapisa-lapisan batubara,
Ply by *ply*	Pengambilan conto batubara pada cara channel sam-ling dimana setia- lapisan disampel secara terpisah
Proksimat	Penentuan pesentase dari kadar kelembaban, zat terbang , karbon tertambat (karbon tetap) dan abu dengan cara tertentu di laboratorium umumnya untuk batubara dan kokas,
Pyrite	Mineral besi sulfida berwarna keemasan atau seperti kuningan yang biasanya terdapatpada lapisan batubara, Pyrite (pirit) merupakan unsur pengotor (sebagai belerang) yang dapat menyebabkan air asam tambang dan gas belerang pada pembangkit listrik,

Pyrite Sulfur	Belerang yang terdapat pada batubara dalam bentuk besi-sulfida, Bersama belerang organis gabungan belerang ini merupakan sumber utama belerang dalam batubara dan dapat merendahkan kualitas batubara,
Reflektansi Vitrinite	Yakni sifat/kemampuan memantulkan cahaya, Sering juga diartikan sebagai
Roof	Batuan di atas lapisan bahan galian; banyak digunakan dalam tambang batubara yang berarti batuan yang terdapat langsung di atas lapisan batubara,
Sapropelic Coal	Sapropelik terbentuk dari tumbuhan tingkat rendah (alga dan jamur),
Seam	Lapisan batubara dengan kata lain suatu pelapisan tipis bila dibandingkan dengan tebalnya batuan di sutu wilayah geologi yang dapat terbagi menjadi 2 atau lebih lapisan dan secara terpisah atau digabung merupakan endapan batubara yang biasanya layak ditambang,
Strike	Garis yang terbentuk karena perpotongan antara bidang datar dengan strata geologi, Dapat juga disebut sebagai bidang datar atau bearing dari pelapisan miring, strata atau urat (vein) ataupun arah garis datar pada bidang lapisan miring batuan, lapisan batubara vein atau gejala (gangguan) geologi,

Subbituminus	Batubara hitam berperingkat antara lignit dan batubara bitumen, berbeda dengan lignit karena mengandung karbon lebih tinggi, hidrogen lebih rendah, Batubara sub-bitumen dibagi atas 3 kelas berdasarkan nilai kalori yang semakin tinggi yaitu c, b dan a,
Subdendritik	Pola aliran yang cabang-cabang sungainya menyerupai struktur pohon,
Sulfat	Bahan pencemar tahap kedua termasuk asam sulfat dan sulfat-sulfat bersifat logam netral,
Sulfur	Unsur atau senyawa belerang yang terdapat dalam batubara berbemtuk pirit atau markasit, belerang organik dan belerang sulfat,
Tissue Preservation Index	TPI atau indeks jaringan terawetkan merupakan maseral yang terawetkan dengan struktur jaringan yang tidak terawetkan atau terdegradasi,
Total Moisture	Kadar lengas (kadar kelembaban/kadar air) yaitu kandungan air permukaan dan atau air tertambat pada batubara dan bahan galian lain,
Total Sulfur	Jumlah belerang dalam batubara yang dinyatakan dalam persen atau bagian dalam sejuta (ppm), Jumlah beelrang ini dapat dibagi tiga, yaitu kandungan belerang pirit, belerang organik dan belerang sulfat
Ultimat	Analisa laboratorium untuk menentukan kandungan abu, karbon, hidrogen, ogsigen dan belerang dalam batubara dengan metoda tertentu,
Underburden	Lapisan tanah (batuan) yang menutupi lapisan batubara bagian bawah, Bila Underburden telah

	digali diangkat dan dibuang disebut waste (limbah),
Upper Delta Plain	Merupakan bagian delta yang berada di atas area pengaruh pasang surut (tidal) dan laut yang signifikan (pengaruh laut sangat kecil),
Vitrinite	Bahan utama penyusun batubara di indonesia (>80 %), Di bawah mikroskop, kelompok maseral ini memperlihatkan warna pantul yang lebih terang dari pada kelompok liptinit, namun lebih gelap dari kelompok inertinit, berwarna mulai dari abu-abu tua hinggga abu-abu terang,
Volatile Matter	Zat terbang (bahan terbang), yaitu zat atau bahan yang keluar (terbang) dari batubara yang dibakar selain dari air yang menjadi uap atau gas, Pembakaran batubara tersebut dilakukan dalam keadaan tertentu (keadaan baku di laboratorium analisis)
Vulkanik	Segala peristiwa yang berhubungan dengan magma yang keluar menuju permukaan bumi melalui rekahan dalam kerak bumi
Wet Forest Swamp	Lingkungan pengendapan gambut yang merupakan ciri lingkungannya rawa air tawar,
XRD	X-Ray Diffraction, teknik analisis yang digunakan untuk menilai kristalinitas dan struktur sampel padat,

Lampiran R. Daftar Singkatan dan lambang

Lambang/Singkatan	**Arti dan Penjelasan**
Ar	*As-Received*
ASTM	*America Society For Testing And Material*
BT	Bujur Timur
Btu/lb	*British Thermal Units Per Pound*
Cly	*Clay*
cm	Centimeter
CV	*Calorific Value*
dmmf	*Dry Mineral matter Free*
FC	*Fixed Carbon*
GCV	*Gross Calorific Value*
GI	*Gelification Index*
IM	*Inherent Moisture*
ISO	*International Organisation For Standardisation*
Kcal/kg	*Kilocalories Per Kilogramme*
LS	Lintang Selatan
m	Meter
mdpl	Meter di atas permukaan laut
MJ/kg	*Megajoules Per Kilogramme*
mm	Milimeter
mmf	*Mineral matter Free*
mmmf	*Moist Mineral matter Free*
NCV	*Net Calorific Value*
Py	*Pyrite*
Qz	Kuarsa
SEM	*Scanning Electron Microscopy*
TM	*Total Moisture*
TPI	*Tissue Preservation Index*
VM	*Volatile Matter*
XRD	*X--Ray Diffraction*

Lambang/Singkatan	**Arti dan Penjelasan**
%	*Percent*
μ	Mikro
μm	Mikrometer
ϴ	*Theta*